Modeling, Simulation and Control of Lower Limb Exoskeleton for Walking on a Flat Surface

Vikash Kumar
Defence Bioengineering and Electromedical Laboratory (DEBEL) Defence Research and Development Organisation (DRDO)
Bangalore, India
vikaskumar.debel@gov.in

Yogesh V. Hote
Department of Electrical Engineering Indian Institute of Technology Roorkee
Roorkee, India
yhotefee@iitr.ac.in

doi: https://doi.org/10.37285/bsp.SACAD2025.69

***Abstract*— The Exoskeletons for human are defined as powered robotic electro-mechanical structures, which exerts an adequate amount of torque/force at human limb joint for normal or enhanced (augmented) limb movement. The mathematical model of such a system exhibits considerable dynamic complexities (large number of DOFs and non-linearity), which requires knowledge of classical mechanics, non-linear mathematics and dynamics. However, for sake of simplicity, a five-link biped is considered as a simplified model of the Exoskeleton. The links are connected by four revolute joints (two at hip and two at the knee). Firstly, the mathematical model of the system is obtained using the Euler - Lagrange method. The beauty of this model is that the approach of modeling is simple to understand and presented in terms of generalized coordinates (relative angles) of the system which is suitable for control system design and analysis. Then the design of the reference trajectory of the system for walking on a flat surface is discussed. Finally, the performance of the dynamic model is evaluated by using the Computed Torque Control (CTC) technique and Classical Sliding Mode Control (SMC).**

Keywords*— Biped, Degree of Freedom (DOF), Lower Limb Exoskeleton, Swing leg, Stance leg, Gait Cycle, Computed Torque Control, Kinematic modeling, Dynamic Modeling.

I. Introduction

The mathematical Model of a robotic system is required for simulation of motion and design of a suitable control system. Simulating the motion of the dynamic robot model enables us to test the control strategies and motion planning methods without the need for a physical system. The Mathematical model is obtained by modeling the exoskeleton theoretically based on the physical characteristics of the system. The major problem to fully describing a locomotion system that imitates human walking is associated with a large number of DOFs and the highly coupled non-linearities involved in the dynamic system, e.g., natural human walking. The first time, T. McGeer carried out the initial studies of the human-like, passive-dynamic walking using a biped robot without actuators and controllers. He showed that a passive biped robot with or without knees can walk smoothly on the downhill slope [1, 2]. Therefore, 5-link Biped system is selected to represent the exoskeleton model with few necessary DOFs to keep the dynamic model at manageable level and yet have sufficient dynamics of interest.

A general 5-link biped modeled as an open kinematic chain with two sub-chains. One sub-chain is called torso, and the other two sub-chains are called legs. Each leg consists of a thigh and a shank link. The joints connecting all sub-chains are termed as hip. The advantage of the Five-link biped model is that it has few DOFs to determine the dynamic mathematical model of its motion and yet still has sufficient DOFs to describe the motion to imitate human-like gait appropriately. For the five-link biped model, feet are considered as mass-less to reduce the complexity in a dynamic model [3, 4]. Fig. 1 represents the biped model in the walking phase with massless feet.

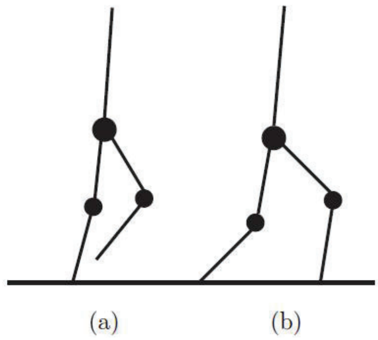

Figure 1. 5 - Link Biped Model (a) Single Support Phase (SSP) (b) Double Support Phase (DSP) [5]

The walking cycle of biped is divided into two-phases (i) Single Support Phase (SSP) (ii) Double Support Phase (DSP). In SSP, only one leg is in contact with the ground, and the contacting leg is known as Stance Leg, while the non-contacting leg is called Swing Leg. The Single Support phase is also referred to as the swing phase. In the Double Support Phase, both legs are in contact with the ground [6]. Then, the alternating phases of single and double support are termed as the biped walking [5].

A planar biped always has motions taking place only in the sagittal plane, whereas a three-dimensional biped walker has motions taking place in both the sagittal and frontal planes.

The sagittal plane divides the body into right and left sections. The frontal plane separates the body into front and back portions. The transverse plane is perpendicular to both the sagittal and frontal planes. The illustration of human plane sections is shown in Fig. 2.

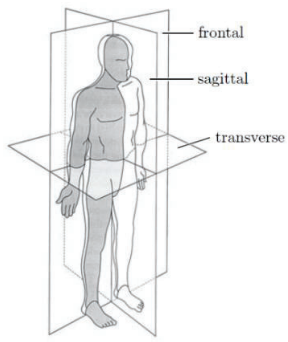

Figure 2. Human plane sections [5]

It is also assumed that during SSP, the stance leg tip act as an ideal joint at ground contact point. Usually, the mathematical model of the robotic system is represented by the equation of motion [7]. The Equation of motion gives a relationship between the joint actuator torques and the motion of the robotic structure as represented in (1).

$$D(\theta)\ddot{\theta} + C(\theta, \dot{\theta})\dot{\theta} + G(\theta) = \tau_\theta \qquad (1)$$

where, $D(\theta)$ is $n \times n$ Inertia matrix, $C(\theta, \dot{\theta})$ is $n \times n$ Coriolis/ centrifugal matrix, $G(\theta)$ is n dimensional Gravity torque vector, τ_θ is the externally applied forces and θ is a set of absolute coordinates. Here n is simply the dimension of above vector, which in case of five link biped is 5.

The above Dynamic equation of motion can be derived using standard procedure of Lagrangian formulation, which is explained in Appendix I.

II. DYNAMICS OF HUMAN LOWER LIMB EXOSKELETON (LLE)

In this section, the human-exoskeleton dynamics are devised by considering a five-link bipedal system in SSP. Further, it is also assumed that the biped system is having a single support motion in a sagittal plane. A schematic representation of the LLE model is shown in Fig. 3 [8].

The LLE model is considered to have massless feet in order to simplify the modeling. Further, it is also assumed that the LLE can apply torque at the ankles even though the dynamics of feet are ignored [9]. Each link of the model shown in Fig. 3 has an associated mass m, moment of inertia I, length L, and the location of its center of mass d. Model parameters related to Fig. 3 are defined in table I.

A. Kinematic Model of Human Exoskeleton in SSP

The biped system, as shown in Fig. 3, consists of five links: a torso and two identical legs with each leg having a thigh and a shank. This biped system has two hip joints and two knee joints. Further, the joints are considered as revolute type and friction-free. It is also assumed that all of the joints are rotating only in the planar (sagittal) plane.

As per the kinematic relationship between the links shown in fig. 3, the position of the center of mass (COM) of each link may be given by equation (2).

Table 1. PARAMETER NOMENCLATURE RELATED TO FIG. 3

Parameter	Description
m_i	Mass of link i
L_i	Length of link i
d_i	Distance between the COM and end of link i
I_i	Moment of inertia of link i
θ_i	Angle of link i with respect to vertical
q_i	Relative angle of link i, where i = 0,1,...4
τ_i	Torque at joint i
x, y	Coordinate reference system

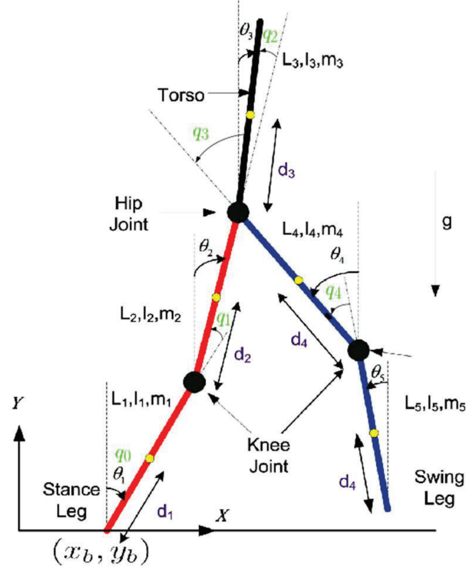

Figure 3. A Planar Five Link Biped Model [8]

$$
\begin{aligned}
x_{COM_1} &= d_1 \sin(\theta_1) \\
y_{COM_1} &= d_1 \cos(\theta_1) \\
x_{COM_2} &= L_1 \sin(\theta_1) + d_2 \sin(\theta_2) \\
y_{COM_2} &= L_1 \cos(\theta_1) + d_2 \cos(\theta_2) \\
x_{COM_3} &= L_1 \sin(\theta_1) + L_2 \sin(\theta_2) + d_3 \sin(\theta_3) \\
y_{COM_3} &= L_1 \cos(\theta_1) + L_2 \cos(\theta_2) + d_3 \cos(\theta_3) \\
x_{COM_4} &= L_1 \sin(\theta_1) + L_2 \sin(\theta_2) + (L_4 - d_4)\sin(\theta_4) \\
y_{COM_4} &= L_1 \cos(\theta_1) + L_2 \cos(\theta_2) - (L_4 - d_4)\cos(\theta_4) \\
x_{COM_5} &= L_1\sin(\theta_1) + L_2\sin(\theta_2) + L_4\sin(\theta_4) \\
&\quad +(L_5 - d_5)\sin(\theta_5) \\
y_{COM_5} &= L_1 \cos(\theta_1) + L_2 \cos(\theta_2) - L_4 \cos(\theta_4) \\
&\quad -(L_5 - d_5)\cos(\theta_5)
\end{aligned}
\qquad (2)
$$

The velocity of the each link's COM in $x - y$ plane is derived by taking the derivative of position for each link's COM.

$$v_{COM_1} = \begin{bmatrix} d_1\, \dot{\theta}_1 \cos(\theta_1) \\ -d_1\, \dot{\theta}_1 \sin(\theta_1) \end{bmatrix}$$

$$v_{COM_2} = \begin{bmatrix} d_2\, \dot{\theta}_2 \cos(\theta_2) + L_1\, \dot{\theta}_1 \cos(\theta_1) \\ -L_1\, \dot{\theta}_1 \sin(\theta_1) - d_2\, \dot{\theta}_2 \sin(\theta_2) \end{bmatrix}$$

$$v_{COM_3} = \begin{bmatrix} d_3\,\dot\theta_3\cos(\theta_3) + L_1\,\dot\theta_1\cos(\theta_1) \\ + L_2\,\dot\theta_2\cos(\theta_2) \\ -L_1\,\dot\theta_1\sin(\theta_1) - L_2\,\dot\theta_2\sin(\theta_2) \\ -\ d_3\,\dot\theta_3\sin(\theta_3) \end{bmatrix}$$

$$v_{COM_4} = \begin{bmatrix} \dot\theta_4\cos(\theta_4)\,(L_4 - d_4) + L_1\,\dot\theta_1\cos(\theta_1) \\ + L_2\,\dot\theta_2\cos(\theta_2) \\ \dot\theta_4\sin(\theta_4)\,(L_4 - d_4) - L_2\,\dot\theta_2\sin(\theta_2) \\ - L_1\,\dot\theta_1\sin(\theta_1) \end{bmatrix} \tag{3}$$

$$v_{COM_5} = \begin{bmatrix} L_1\,\dot\theta_1\cos(\theta_1) + L_2\,\dot\theta_2\cos(\theta_2) + L_4\,\dot\theta_4\cos(\theta_4) \\ + \dot\theta_5\cos(\theta_5)\,(L_5 - d_5) \\ -L_1\,\dot\theta_1\sin(\theta_1) - L_2\,\dot\theta_2\sin(\theta_2) + L_4\,\dot\theta_4\sin(\theta_4) \\ + \dot\theta_5\sin(\theta_5)\,(L_5 - d_5) \end{bmatrix}$$

The position of the swing leg's end point of biped model is given as

$$x_{SL_{tip}} = L_1\sin(\theta_1) + L_2\sin(\theta_2) + L_4\sin(\theta_4) + L_5\sin(\theta_5) \tag{4a}$$

$$y_{SL_{tip}} = L_1\cos(\theta_1) + L_2\cos(\theta_2) - L_4\cos(\theta_4) - L_5\cos(\theta_5) \tag{4b}$$

The equations (2) & (3) are used to derive the dynamic model of the human exoskeleton (Biped Model) in next sub-section.

B. Dynamic Model of Human Lower Limb Exoskeleton

The differential equations of the dynamic motion of Biped model are derived using Euler-Lagrangian equation of motion as per Eq. (7) given at Appendix A. The dynamics of a five link biped system is complex, therefore dynamic model of biped system is derived using **Symbolic Math Toolbox** of **MATLAB**.

The detailed procedure of deriving the equation of motion is presented at Appendix B. Each term in (1) is formulated as follows:

$$\begin{aligned} \theta &= [\theta_1 \quad \theta_2 \quad \theta_3 \quad \theta_4 \quad \theta_5]^T, \\ \tau_\theta &= [\tau_{\theta_1} \quad \tau_{\theta_2} \quad \tau_{\theta_3} \quad \tau_{\theta_4} \quad \tau_{\theta_5}]^T, \\ D(\theta) &= [D_{ij}(\theta)], \\ C(\theta,\dot\theta) &= [C_{ij}(\theta,\dot\theta)], \\ G(\theta) &= col[G_i(\theta)]\ (i,j = 1,2....5) \end{aligned} \tag{5}$$

Where, τ_{θ_i} is the torque corresponding to angle θ_i. The elements of $D(\theta)$, $C(\theta,\dot\theta)$ and $G(\theta)$ are selected as given in Appendix 8. It is noted here that only four of the five degree of freedoms have to be controlled directly by the four driving torques at the four joints. The angle θ_1 at the ground contact point is controlled indirectly using the gravitational effect [10]. Now considering the $\tau = [\tau_1 \quad \tau_2 \quad \tau_3 \quad \tau_4]^T$ be the vector of driving torques of the four joints of the exoskeleton, where τ_1 is the driving torque of knee joint of the stance leg, τ_2 is the driving torque of the the hip joint of stance leg, τ_3 is the driving torque of hip joint of the swing leg and τ_4 is the driving torque of the knee joint of the swing leg.

If q_1, q_2, q_3 and q_4 are the relative angles of the corresponding joints, then by referring the Fig. 3, the relationship between relative joint and absolute joint is as follows:

$$\begin{aligned} q_0 &= \theta_1; \quad q_1 = \theta_1 - \theta_2; \quad q_2 = \theta_2 - \theta_3; \\ q_3 &= \theta_3 + \theta_4; \quad q_4 = \theta_4 - \theta_5. \end{aligned} \tag{6}$$

In order to facilitate the control procedure, the equation of motion (1) needs to be transformed in terms of relative angles between links as

$$D_q(q)\ddot q + C_q(q,\dot q)\dot q + G_q(q) = \tau_q \tag{7}$$

where, $\tau_q = [\tau_{q_0} \quad \tau_{q_1} \quad \tau_{q_2} \quad \tau_{q_3} \quad \tau_{q_4}]^T$ and $q = [q_0 \quad q_1 \quad q_2 \quad q_3 \quad q_4]^T$. A transformation to express the q by θ can be given as

$$q = T_{q\theta}.\theta \tag{8}$$

where, $T_{q\theta}$ is a transformation matrix from θ to q:

$$T_{q\theta} = \begin{bmatrix} 1 & 0 & 0 & 0 & 0 \\ 1 & -1 & 0 & 0 & 0 \\ 0 & 1 & -1 & 0 & 0 \\ 0 & 0 & 1 & 1 & 0 \\ 0 & 0 & 0 & 1 & -1 \end{bmatrix}$$

The relation between the segment and joint torques is [11]

$$\tau_{\theta_i} = \sum_{j=1}^5 \tau_{j-1}\frac{\partial q_{j-1}}{\partial \theta_i} = \sum_{j=1}^5 \tau_{j-1}\,(T_{q\theta})_{ji} \tag{9}$$

Equation (9) can be represented in vector form as

$$\begin{aligned} \tau_\theta &= (\tau_q^T\,T_{q\theta})^T = T_{q\theta}^T\,\tau_q \\ or\ \tau_q &= (T_{q\theta}^T)^{-1}.\tau_\theta \end{aligned} \tag{10}$$

Thus, the generalized torques τ_{q_i} that correspond to variable $q_i (i = 0,1,....,4)$ are:

$$\tau_q = \begin{bmatrix} \tau_{q_0} \\ \tau_{q_1} \\ \tau_{q_2} \\ \tau_{q_3} \\ \tau_{q_4} \end{bmatrix} = \begin{bmatrix} 0 \\ \tau_1 \\ \tau_2 \\ \tau_3 \\ \tau_4 \end{bmatrix} = \begin{bmatrix} \tau_{\theta_1} + \tau_{\theta_2} + \tau_{\theta_3} - \tau_{\theta_4} - \tau_{\theta_5} \\ -\tau_{\theta_2} - \tau_{\theta_3} + \tau_{\theta_4} + \tau_{\theta_5} \\ -\tau_{\theta_3} + \tau_{\theta_4} + \tau_{\theta_5} \\ \tau_{\theta_4} + \tau_{\theta_5} \\ -\tau_{\theta_5} \end{bmatrix}$$

In order to solve the coefficient matrix terms for (7), substitute (8) and (10) into (1), the following transformation forms can be determined,

$$D_q = (T_{q\theta}^{-1})^T\,D_\theta(\theta(q))\,T_{q\theta}^{-1} \tag{11a}$$

$$C_q = (T_{q\theta}^{-1})^T\,C_\theta(\theta(q),\dot\theta(\dot q))\,T_{q\theta}^{-1} \tag{11b}$$

$$G_q = (T_{q\theta}^{-1})^T\,G_\theta(\theta(q)) \tag{11c}$$

Even though torque τ_{q_0} is hypothetically described as being equal to zero, there exists a resistive passive torque at joint (q_0) which must be compensated for by the controller. $D(q)$ should be invertible. The elements of D_q, C_q and G_q are given at Appendix C.

C. Support End Phase Transition

Locomotion of Exoskeleton is defined by a continuous sequence of phase transitions from DSP to SSP, SSP to DSP, and so on. At the end of the single support phase (SSP), the swing leg comes into immediate contact with the ground surface. At this moment, the role of support end is transferred to the tip of the swing leg, and the support leg, which now becomes swing leg, leaves the walking surface. Due to the collision with the ground (walking) surface, there exists an instantaneous change (discontinuities) in the angular velocities of each joint. This implies that at the moment of collision, support (stance) leg tip constraint $x_b = y_b = constant$ and $\dot{x}_b = \dot{y}_b = 0$ is no longer valid. Therefore, the dynamic model of the SSP phase (8) can not be used to compute the instantaneous change in the angular velocities of each joint. This demands the derivation of the dynamic model of the double support phase to compute the sudden changes in angular velocities at the moment of swing leg tip contact with the ground.

However, this study concentrates on the efficacy of augmentation of the soldier's lower limb movement, which shall be achieved via a wearable robotic Exoskeleton controlled by real-time measured gait data of the wearer. Since the human gait shall be used to actuate the joints, calculation of the angular velocities before and after impact is eliminated here as the transition shall be automatic.

As discussed above, the roles of the swing leg and support leg has to be exchanged after each step. Therefore, the numbering of links has to be relabeled to use the same equation of motion of the single support phase for both legs. The relabeling scheme is as follows:

Link 1 ↔ Link 5, Link 2 ↔ Link 4,
Link 3 does not change

Since in this study, human-like walking of the symmetrical dynamic model for SSP with a suitable controller is simulated, joint angle profiles computed for a single step are repeated at predetermined intervals.

Therefore, relabeling of links in model and use of single step joint profiles lead to the following changes in initial angular displacement of the next step.

$$\theta_{1_{NS}}(0) = -\theta_{5_{PS}}(T), \quad \theta_{2_{NS}}(0) = -\theta_{4_{PS}}(T),$$
$$\theta_{3_{NS}}(0) = \theta_{3_{PS}}(T), \quad \theta_{4_{NS}}(0) = -\theta_{2_{PS}}(T),$$
$$\theta_{5_{NS}}(0) = -\theta_{1_{PS}}(T),$$

where, NS is next step, PS is previous step, $\theta_i(0)$ is initial joint angle condition of next step and $\theta_i(T)$ is the terminal posture of the completion of each step. The initial conditions for angular velocities for next step are set to zero.

The transformation matrix for the relative joint profile can be obtained from the above relationships. The absolute angle in terms of relative angles as per equation (8) are as follows:

$$\begin{aligned}
\theta_1(0) &= q_0(0) \\
\theta_2(0) &= q_0(0) - q_1(0) \\
\theta_3(0) &= q_0(0) - q_1(0) - q_2(0) \\
\theta_4(0) &= -q_0(0) + q_1(0) + q_2(0) + q_3(0) \\
\theta_5(0) &= -q_0(0) + q_1(0) + q_2(0) + q_3(0) - q_4(0)
\end{aligned}$$

Now, the initial conditions for relative joint angle can be determine as follows:

$$\begin{aligned}
q_0(0) &= \theta_1(0) = -\theta_5(T) \\
&= q_0(T) - q_1(T) - q_2(T) - q_3(T) + q_4(T) \\
q_1(0) &= \theta_1(0) - \theta_2(0) = -\theta_5(T) + \theta_4(T) = q_4(T) \\
q_2(0) &= \theta_2(0) - \theta_3(0) = -\theta_4(T) - \theta_3(T) = -q_3(T) \quad \ldots (12) \\
q_3(0) &= \theta_3(0) + \theta_4(0) = -\theta_3(T) - \theta_2(T) = -q_2(T) \\
q_4(0) &= \theta_4(0) - \theta_5(0) = -\theta_2(T) + \theta_1(T) = q_1(T)
\end{aligned}$$

In matrix form, it is represented as

$$\begin{bmatrix} q_0(0) \\ q_1(0) \\ q_2(0) \\ q_3(0) \\ q_4(0) \end{bmatrix} = \begin{bmatrix} 1 & -1 & -1 & -1 & 1 \\ 0 & 0 & 0 & 0 & 1 \\ 0 & 0 & 0 & -1 & 0 \\ 0 & 0 & -1 & 0 & 0 \\ 0 & 1 & 0 & 0 & 0 \end{bmatrix} \begin{bmatrix} q_0(T) \\ q_1(T) \\ q_2(T) \\ q_3(T) \\ q_4(T) \end{bmatrix} \tag{13}$$

The new angular displacements (joint angles) calculated from above equation are used as initial condition for the next step.

III. TRAJECTORY GENERATION

To carry out the dynamic analysis of the Exoskeleton mathematical model, one needs joint angle trajectories. The human gait data contains the ideal joint trajectories for this type of study. However, in the absence of readily available gait data, there is a inescapable need to synthesize a cyclic gait for walking. Here, the approach used for gait generation is similar to techniques used for Biped gait synthesis. Many researchers have studied the systematic approach for generating biped gait. The method of using objective functions in association with a suitable controller to regulate the locomotion of five-link biped is widely used approach. As per this technique, biped motions are designed in terms of step length, progression speed, maximum step height, and the stance knee bias angle. However, to have cyclic gait, the selection of the initial gait parameters and objective functions are exceptionally challenging.

One of the possible solution to the above challenge of selecting an objective function and initial joint angles is to use time cubic or quintic polynomial. However, the selection of an improper order of polynomials may lead to undesirable features of gait.

The bipedal walking locomotion synthesize using the desired joint angle profile shall have repeatability characteristics of human walking. Therefore, the designed joint angles must ensure the repeatability condition for steady and continuous walking. For simplicity, the problem of synthesizing the gait is divide into two parts. Swing leg tip and hip trajectories are designed first. Based on designed hip and swing leg tip trajectories, joint angles profile are computed using inverse kinematic analysis.

However, the hip and swing leg tip trajectories must satisfy the two condition as follows:

1. ***Condition 1:*** The distance between the hip and each lower limb tip is less than the length of the entire limb and higher than the difference between the length of the thigh and shank limb.
2. ***Condition 2:*** The knee of both legs must bend only in one direction (Knee extension).

The above two conditions ensure the existence of the uniqueness of a joint angle profile determined from the trajectories of hip and swing leg tip. The walking cycle should be in the sagittal plane as depicted in Fig. 4. For a natural human-like walking, the torso is maintained directly upward or oscillates slightly around the upright position [12], [13].

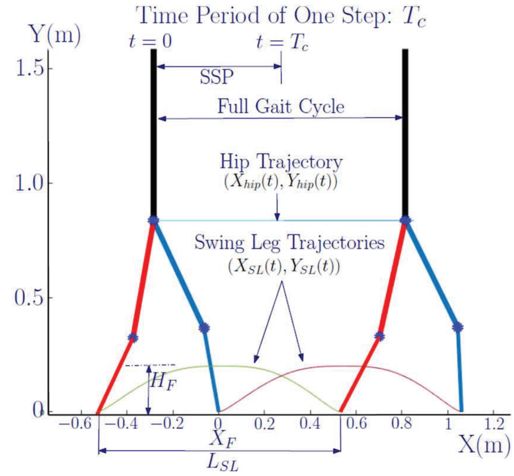

Figure 4. Gait cycle design in sagittal plane

A. Design of Swing Leg Trajectory

The primary requirement of the swing phase of the gait cycle is that the swing leg tip must be clear of the walking surface after the leg take off from the surface and before landing on the surface. The trajectory of the swing leg tip is denoted by $(X_{SL}(t), Y_{SL}(t))$, where $X_{SL}(t)$ and $Y_{SL}(t)$ are the coordinate of the swing leg tip position in Cartesian space as shown in the Fig. 4. Origin of the coordinate system is located at the tip of the stance leg. The ground clearance condition of the swing leg is satisfied by selecting the cubic and quintic polynomial functions for the $X_{SL}(t)$ and $Y_{SL}(t)$, respectively. If T_c denotes the time duration of SSP, then the polynomial for the coordinates of the swing leg tip is generated as

$$X_{SL}(t) = a_0 + a_1 t + a_2 t^2 + a_3 t^3, \quad 0 \le t \le T_c \tag{14a}$$

$$Y_{SL}(t) = b_0 + b_1 t + b_2 t^2 + b_3 t^3 + b_4 t^4 + b_5 t^5, 0 \le t \le T_c \tag{14b}$$

The coefficients of the polynomials given in equation (14) are computed by defining the constraints on $(X_{SL}(t), Y_{SL}(t))$ and their derivatives [7]. These constraints are inferred from the condition of the desired gait cycle for locomotion. The primary conditions characterizing the gait pattern are:

- Step length L_{SL}
- SSP Step period T_c
- Maximum clearance of swing leg from walking surface H_F
- Location of Maximum clearance X_F

The repeatable and continuous gait cycle is achieved using the constraints relations defined as below:

a) Initial and final value constraints

The repeatable gait patterns demands that the Posture and velocities must be identical at the start of step (initial) and the end of each step. Posture repeatability is ensured by making identical strides. This condition results in the following constraints:

$$X_{SL}(0) = -\frac{L_{SL}}{2}, \quad X_{SL}(T_c) = \frac{L_{SL}}{2} \tag{15}$$

Since the swing leg has to be lifted off the walking surface at the starting of the cycle and has to land back at the end of SSP. This condition results in the following equations.

$$Y_{SL}(0) = 0, \quad Y_{SL}(T_c) = 0 \tag{16}$$

Furthermore, at the start of each step, initial velocities of swing leg in horizontal and vertical direction must be zero to keep gait repeatability.

$$\dot{X}_{SL}(0) = 0, \quad \dot{Y}_{SL}(0) = 0 \tag{17}$$

b) Maximum clearance of the swing limb

The condition of avoiding the contact of the swing leg with the walking surface during the swing phase is ensured by following equations.

$$X_{SL}(T_F) = X_F, \quad Y_{SL}(T_F) = H_F, \quad \dot{Y}_{SL}(T_F) = 0 \tag{18}$$

where, H_F is the maximum clearance of the swing leg and X_F is the position of swing leg on X-axis corresponding to the maximum clearance. T_F is the time required to reach the maximum clearance.

c) Continuity of the Gait Cycle

The transition between the swing leg and stance leg role should be continuous. The impact of swing leg on the ground causes a sudden change in joint angular velocities. The discontinuities in joint angular velocities will be lower if the velocity of the swing leg tip is low. Therefore joint angular velocities discontinuities can be eliminated if swing leg tip velocity is set to zero before impact. This condition results in following equation.

$$\dot{X}_{SL}(T_c) = 0, \quad \dot{Y}_{SL}(T_c) = 0 \tag{19}$$

B. Design of Trajectory of Hip

The trajectory of the hip is denoted by $(X_{hip}(t), Y_{hip}(t))$, where $X_{hip}(t)$ and $Y_{hip}(t)$ are the coordinate of the hip position in Cartesian space, as shown in the Fig. 4. The coordinates of the hip position in Cartesian space are described by the following function.

$$\begin{aligned} X_{hip}(t) &= d_0 + d_1 t + d_2 t^2 + d_3 t^3 \quad 0 \le t \le T_c, \\ Y_{hip}(t) &= y_h(t) \quad 0 \le t \le T_c \end{aligned} \tag{20}$$

The coefficients of the (20) are computed using constraints, formulated based on the position of hip at the beginning of the SSP and the height of the hip. The initial and final value constraints on $X_{hip}(t)$ are defined as:

$$\begin{aligned} X_{hip}(0) &= -x_{hip}, \quad X_{hip}(T_c) = x_{hip}, \\ \dot{X}_{hip}(0) &= 0, \quad \dot{X}_{hip}(T_c) = 0, \end{aligned} \tag{21}$$

In order to synthesize the stable walking cycle, the vertical motion of the hip is needed to be keep minimum. This condition is enforced by assuming that Y_{hip} is constant at any given time during the complete gait cycle as follows:

$$Y_{hip}(t) = y_h(t) = H_{hip} \tag{22}$$

where, H_{hip} is the height of hip from the walking surface.

ISBN: 978-93-47311-06-2

C. Joint Angle Profile Computation

The angular displacement of joints of the Exoskeleton are computed utilizing inverse kinematics analysis. Swing Leg and hip trajectories are used as input to generate joint variables. Joint variables are determined using the geometric approach of Inverse Kinematic. Joint angles or variables associated with 5 - link robotic model of Exoskeleton are shown in Fig 3. For the sake of simplicity and smoothness of locomotion, the body maintains an erect posture i.e., the absolute angle of the torso (θ_3) is maintained at 0 deg. By utilizing the geometric approach, the joint variables associated with Lower limb, as shown in Fig. 5 are computed as follows:

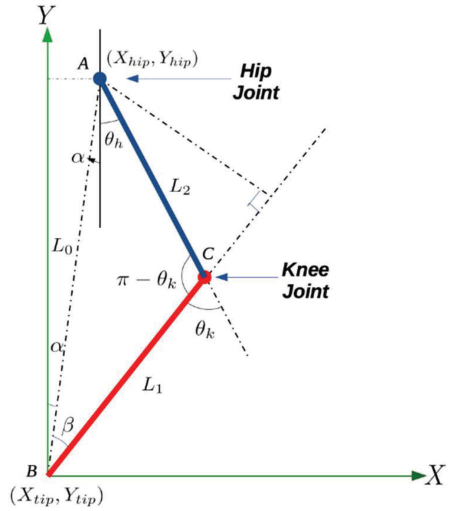

Figure 5. Geometric Inverse Kinematic Analysis of Lower Limb of Exoskeleton

$$L_0 = \sqrt{(X_{hip} - X_{tip})^2 + (Y_{hip} - Y_{tip})^2}$$

Using Cosine rule for triangle ABC,

$$\cos(\pi - \theta_k) = \frac{L_1^2 + L_2^2 - L_0^2}{2L_1L_2} \Rightarrow \cos(\theta_k) = \frac{L_0^2 - L_1^2 - L_2^2}{2L_1L_2}$$

$$\theta_k = \cos^{-1}\left(\frac{L_0^2 - L_1^2 - L_2^2}{2L_1L_2}\right) \quad (23)$$

Using sine rule

$$\frac{\sin\beta}{L_2} = \frac{\sin(\pi - \theta_k)}{L_0} \Rightarrow \beta = \sin^{-1}\left(\frac{L_2\sin(\pi - \theta_k)}{L_0}\right) \quad (24)$$

$$\frac{\sin\alpha}{X_{hip} - X_{tip}} = \frac{\sin(\pi/2)}{L_0} \Rightarrow \alpha = \sin^{-1}\left(\frac{X_{hip} - X_{tip}}{L_0}\right) \quad (25)$$

By taking the sum of angles in $\triangle ABC$, we determine the $\angle\theta_h$

$$\alpha + \theta_h + \pi - \theta_k + \beta = \pi \Rightarrow \theta_h = \theta_k - \alpha - \beta \quad (26)$$

Now the joint variable for stance, swing leg and torso of model shown in Fig. 3 can be estimated by using the relations derived in (23), (24) and (26).

1) Stance Leg Joint variables

In case of stance leg, the coordinates of tip are constant i.e. (0,0) for complete duration of the cycle. However, the hip trajectory is given by (20). As per the Fig. 5, the joint variables of stance leg are computed as follow:

$$\theta_1 = \alpha + \beta, \qquad \theta_2 = -\theta_h \quad (27)$$

2) Torso Joint Variable

Since the torso is kept in upright erect position to achieve human-like gait, absolute angle of torso joint is given as follow:

$$\theta_3 = 0 \quad (28)$$

3) Swing Leg Joint variables

By using the trajectories of swing leg (14) and hip (20) as coordinated of the limb tip and hip of as shown in Fig. 5, absolute joint angles of swing leg are computed as follows:

$$\theta_4 = \theta_h, \theta_5 = -(\alpha + \beta) \quad (29)$$

4) Relative Joint Angles Profile of Exoskeleton

By using the (8), absolute joint angle profiles computed by equations from (27) to (29) can be transformed in to relative joint angle profiles as follows:

$$\begin{aligned} q_0 &= \theta_1, \quad & q_1 &= \theta_1 - \theta_2, \quad & q_2 &= \theta_2 - \theta_3 \\ q_3 &= \theta_3 + \theta_4, \quad & q_4 &= \theta_4 - \theta_5 \end{aligned} \quad (30)$$

IV. CONTROL OF LOWER LIMB EXOSKELETON (LLE)

A controller for dynamic model of LLE, given by (7), must be designed so that the controller output drives the actual trajectories of the system to reference trajectories in the presence of system non-linearity, parametric uncertainty, and external disturbance.

Here, the study and performance comparison of the Computed Torque Control and Sliding Mode Control is carried out, when applied to the LLE locomotion.

A. Computed Torque Control

Computed-Torque control is a standard technique used for the model based control of nonlinear MIMO Robotic Systems [14, 15]. This technique sometimes referred to as feedback linearisation, which utilises the control law partitioning scheme. Fig. 6 shows the block diagram of a closed loop model-based control system. The concept of the said Computed-Torque control is discussed below.

For a MIMO robotic system, we have vector of desired joint positions, velocities, and acceleration. The basic control law partitioning scheme can be used here in matrix-vector form. The model based portion is given by [16].

$$F = \alpha F' + \beta \quad (31)$$

where, for n DOFs system, F, F' and β are $n \times 1$ vectors and α is $n \times n$ matrix.

The servo law for MIMO system [16]

$$F' = \ddot{X}_d + K_d\dot{E} + K_pE \quad (32)$$

where, K_d, K_p are $n \times n$ diagonal matrix. $\dot{E}$, E are $n \times 1$ error vector in term of velocity and position. The rigid body dynamics is given by

$$D_q(q)\ddot{q} + C_q(q,\dot{q})\dot{q} + G_q(q) = \tau_q \quad (33)$$

By partitioning control scheme,

$$\tau = \alpha\tau' + \beta \quad (34)$$

where, τ is $n \times 1$ vector of joints torques. If we select,

$$\begin{aligned} \alpha &= D_q(q) \\ \beta &= C_q(q,\dot{q})\dot{q} + G_q(q) \end{aligned} \tag{35}$$

By equating Eq (37) and Eq. (38), we get

$$\ddot{q} = \tau' \tag{36}$$

then servo control law is given by

$$\tau' = \ddot{q}_d + K_d\dot{E} + K_pE \tag{37}$$

where, $E = q_d - q$ and $\dot{E} = \dot{q}_d - \dot{q}$.

Using the above Equations from (33) to (37) the closed loop system is characterized by the 2^{nd} order error dynamic [16]

$$\ddot{E} + K_d\dot{E} + K_pE = 0 \tag{38}$$

This vector equation is decoupled by diagonal matrix K_p, K_d and Eq. (38) can be written for i^{th} joint.

$$\ddot{e}_i + K_d\dot{e}_i + K_pe_i = 0 \tag{39}$$

If the matrices K_p and K_d are positive definite then the tracking error $E(t)$ tends to zero asymptotically as $t \to \infty$. If λ is the desired bandwidth then, to ensure a critically damped closed loop performance, the gain matrices K_p & K_d are selected as follows:

$$\begin{aligned} K_p &= diag[\lambda^2] \\ K_d &= diag[2\lambda] \end{aligned} \tag{40}$$

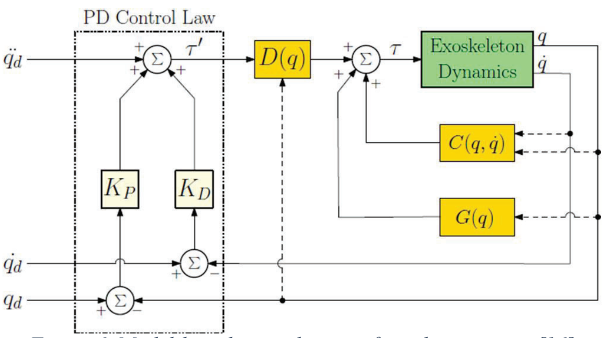

Figure 6. Model-based control system for robotic system [16]

B. Sliding Mode Control (SMC)

Parametric uncertainty, un-modeled dynamics, and external disturbance degrade the performance on the non-linear control system. One approach to address this issue is to implement a Robust controller. Sliding mode control is one class of such Robust controller. The typical SMC structure is comprised of a nominal part, similar to Computed Torque Control Law, and an additional part focused on dealing with uncertainty and external disturbance. The implementation of SMC is based on constructing a mathematical surface known as a sliding surface with the property that the system trajectories are confined to the sliding surface. Such time-varying surface $S(t)$ in the state-space for tracking error vector $e = q - q_d$ is defined by scalar equation $s(q;t) = 0$, where

$$s(q;t) = \left(\frac{d}{dt} + \lambda\right)^{n-1} e \tag{41}$$

For second order system ($n = 2$), $s = \dot{e} + \lambda\, e$, where λ is a positive constant and $\dot{e} = \dot{q} - \dot{q}_d$.

The integral control action is implemented, if integral term $\int_0^t e(\tau)d\tau$ is considered variable of interest instead of e [17]. The time-varying surface for $n = 3$ becomes

$$\begin{aligned} s &= \left(\frac{d}{dt} + \lambda\right)^2 \left(\int_0^t e(\tau)d\tau\right) \\ &= \dot{e} + 2\lambda e + \lambda^2 \int_0^t e(\tau)d\tau \end{aligned} \tag{42}$$

The dynamics during sliding mode is given by $\dot{s} = 0$. The time derivative of (42) in form of (7) is given as

$$\begin{aligned} \dot{s} &= \ddot{e} + 2\lambda\dot{e} + \lambda^2 e = \ddot{q} - \ddot{q}_d + 2\lambda\dot{e} + \lambda^2 e \\ &= D_q^{-1}\left(\tau_q - C_q(q,\dot{q})\dot{q} - G_q(q)\right) - \ddot{q}_d + 2\lambda\dot{e} + \lambda^2 e \end{aligned} \tag{43}$$

By solving the above equation as $\dot{s} = 0$ for control input, we get an equivalent control law as

$$\tau_{q_{eq}} = D_q(\ddot{q}_d - 2\lambda\dot{e} - \lambda^2 e) + C_q(q,\dot{q})\dot{q} + G_q(q) \tag{44}$$

This control action is considered as continuous control law, which is similar to computed torque control. To deal with uncertainty on dynamics, a discontinuous term across $s = 0$ is added to $\tau_{q_{eq}}$:

$$\tau = \tau_{q_{eq}} - k\, sgn(s) \tag{45}$$

where, sgn is the sign function

$$sgn(s) = +1 if\ s > 0$$
$$sgn(s) = -1 if\ s < 0$$

and k is constant, selected large enough so that following relationship is verified.

$$\frac{1}{2}\frac{d}{ds}s^2 \le -\eta|s| \tag{46}$$

where, η is strictly positive constant. If σ is the bound on the system dynamic estimation, then k is given by $k = \sigma + \eta$.

The discontinuous control law (45), ensuring the perfect tracking in the presence of uncertainty, ideally need infinite switching frequency. However, finite time computation of the controller and the finite bandwidth of actuator leads to the phenomenon known as chattering, which involves extremely high control activity. Solution to eliminate the chattering can be achieved by smoothing out the control discontinuity in a thin boundary layer neighboring the switching surface [17].

$$B(t) = \{q, |s(q;t)| \le \phi\}\phi > 0 \tag{47}$$

where, ϕ is the boundary layer thickness given by $\phi = \epsilon\, \lambda^{n-1}$, while ϵ being the boundary layer width. This leads perfect tracking to within a guaranteed precision ϵ. For all trajectories starting inside $B(t = 0)$

$$\forall\ t \ge 0,\ \ |e^i(t)| \le (2\lambda)^i\epsilon, \quad i = 0, \ldots. n - 1$$

The modified control law [17] in thin boundary layer of thickness ϕ is given as

$$\tau = \tau_{q_{eq}} - k\, sat(s/\phi) \tag{48}$$

where sat is the saturation function

$$sat(x) = x if \qquad |x| \le 0$$

$$sat(x) = sgn(x) \quad otherwise$$

V. Numerical Simulation

In this section, the simulation of the 5-link Exoskeleton dynamic model is presented. The physical parameters for dynamic models are given in table 2. The parameters given here are considered for a person with a weight of $65kg$ [18].

MATLAB R2015b software running on a PC (Intel(R) CORE(TM) i7 3.40 GHz processor with 16GB RAM) is used to carry out the simulations.

The simulation is undertaken in two cases:

Case 1 :– Computed torque control simulation with no external disturbance

Case 2 :– CTC and SMC in presence of external disturbance

TABLE II. Physical Parameters of Biped Model [18]

Parameters	Values
$m_{1,5}$	$3.02\ kg$
$m_{2,4}$	$6.50\ kg$
m_3	$44.07\ kg$
$L_{1,5}$	$0.37\ m$
$L_{2,4}$	$0.52\ m$
L_3	$0.75\ m$
$d_{1,5}$	$0.19\ m$
$d_{2,4}$	$0.26\ m$
d_3	$0.38\ m$
$I_{1,5}$	$0.28\ kg.m^2$
$I_{2,4}$	$1.17\ kg.m^2$
I_3	$16.53\ kg.m^2$
g	$9.8\ m/s^2$

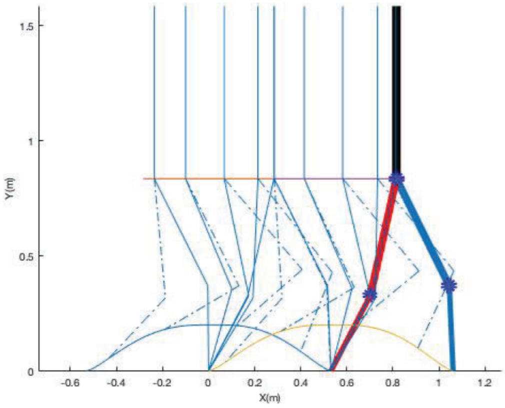

Figure 7. Exoskeleton Dynamic simulation stick diagram for Case 1

A. Case 1: – Computed torque control with no external disturbance

Simulation of LLE is carried out using PD law based on computed torque control technique. The value of gain matrix is given below.

$$K_p = diag([100 \quad 100 \quad 100 \quad 100 \quad 100]) \\ K_d = diag([20 \quad 20 \quad 20 \quad 20 \quad 20]) \tag{49}$$

The values of gain matrix are selected in order to achieve best tracking of the desired trajectories.

The physical parameters are taken as per table 2. The initial relative joint angles in deg are $q_0 = -10$, $q_1 = 15$, $q_2 = -25$, $q_3 = -10$ & $q_4 = 15$ and initial joint velocities are set to zero.

The results of simulation are given below in fig. 8, 9, 10, 11, 12 & 13. Exoskleton simulation stick diagram for full gait cycle is shown in Fig. 7. Fig. 8 to 12 shows the tracking of desired trajectories for each joint angles. Fig. 13 shows the torque applied at each link segments and joint angle tracking error.

In fig. 13, highest joint torque is observed for knee joint of stance leg. This is due to the fact that during swing phase whole body weight is being transferred to ground through stance leg and more efforts are required by stance leg to achieve the locomotion.

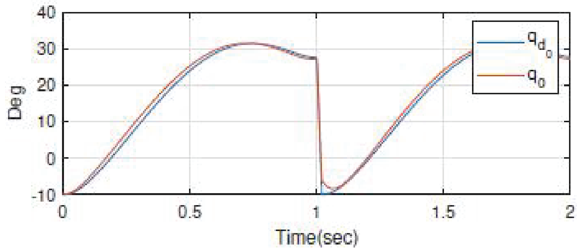

Figure 8. Tracking of desired relative angle q_0 for Case 1

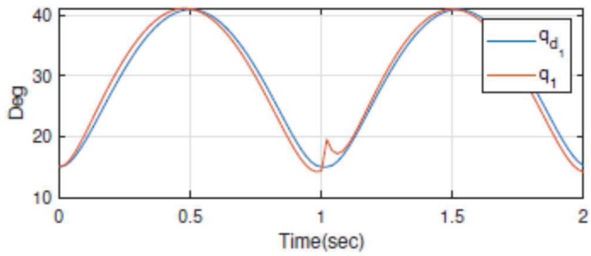

Figure 9. Tracking of desired relative angle q_1 for Case 1

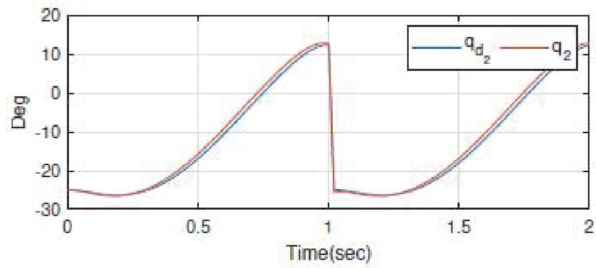

Figure 10. Tracking of desired relative angle q_2 for Case 1

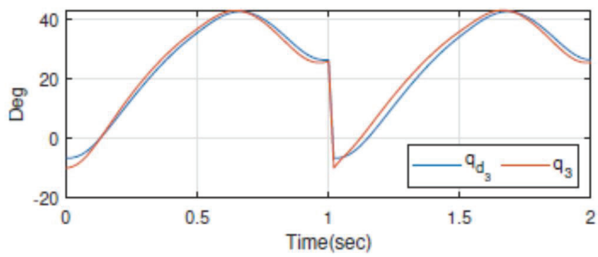

Figure 11. Tracking of desired relative angle q_3 for Case 1

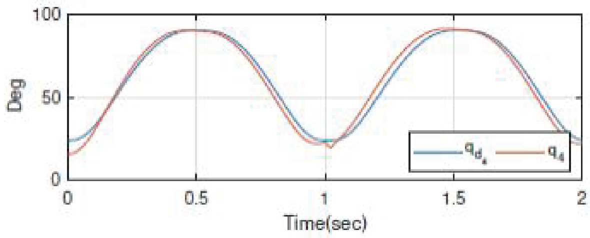

Figure 12. Tracking of desired relative angle q_4 for Case 1

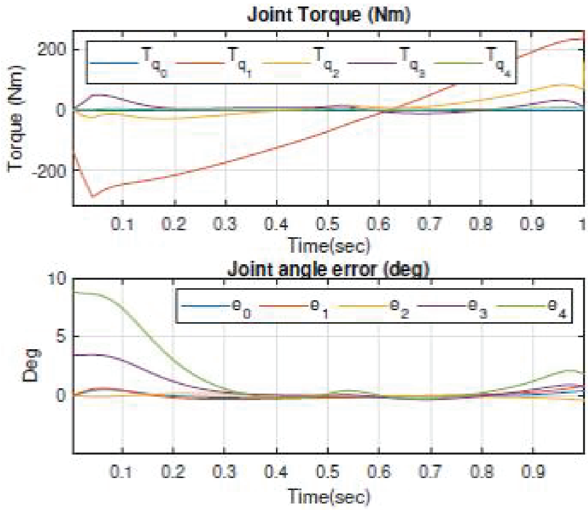

Figure 13. Joint torque and Joint angle error of biped one step locomotion in SSP for Case 1

B. Case 2: – CTC and SMC in presence of external disturbance

In case 2, the performance of CTC and SMC is compared in presence of an external disturbance Torque signal. The disturbance torque signal is designed in the form of a sinusoidal signal with a switching function. This disturbance is given by (50) and shown in Fig.14.

$$\tau_{dist} = 10sin(6\pi t)[sign(\dot{q}_d)] \quad (50)$$

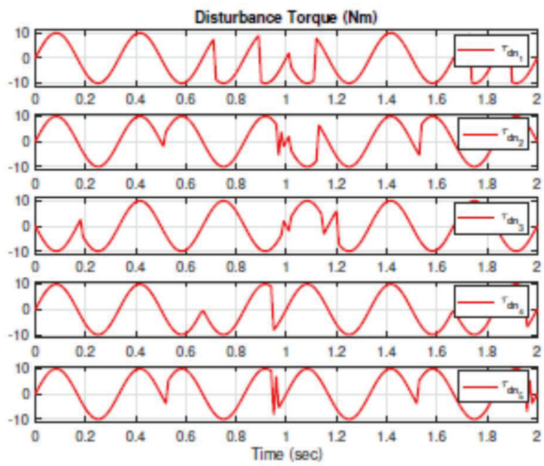

Figure 14. Disturbance Torque for Each joint for Case 2

Simulation results using CTC and SMC technique in the presence of external torque disturbance are presented here, respectively. The gain parameters of the controller for simulation is the same as used in Case 1.

Fig. 15 represents the stick diagram of one Gait cycle locomotion of LLE using CTC in presence of external disturbance torque. It is clearly evident from the Fig 15 that CTC controller is not able to track the desired swing leg trajectory. The joint angle errors for this controller are shown in Fig. 16.

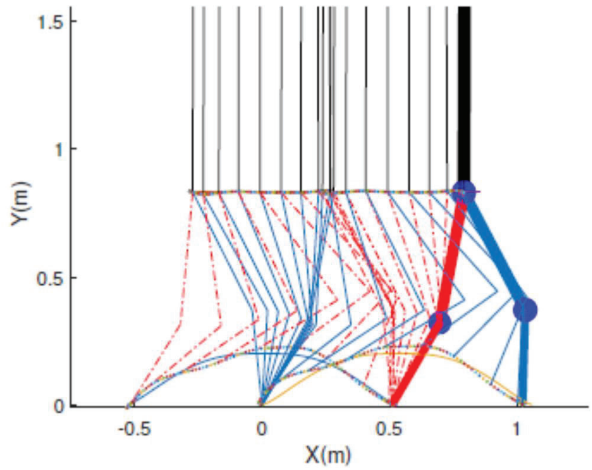

Figure 15. Stick Diagram of LLE using CTC for Case 2

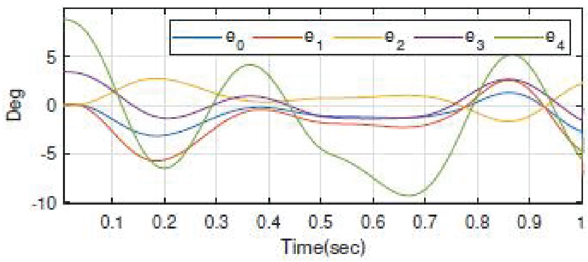

Figure 16. Joint Angle Error using CTC for Case 2

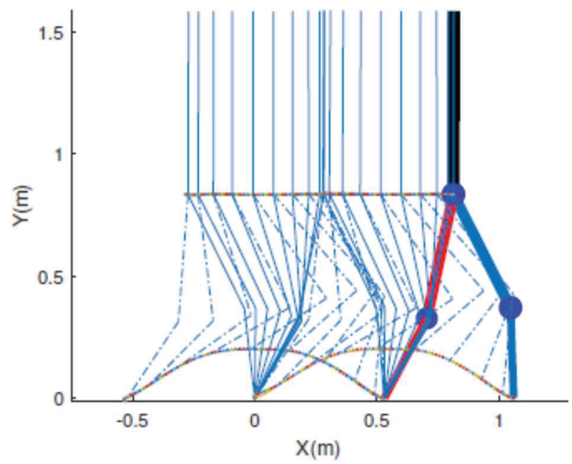

Figure 17. Stick Diagram using SMC for Case 2

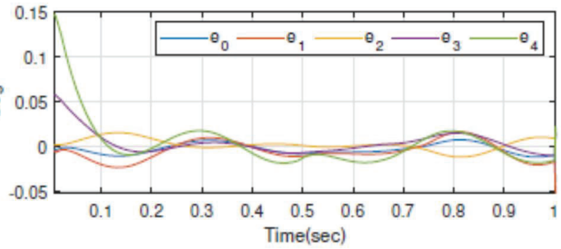

Figure 18. Joint Angle Error using SMC for Case 2

For simulation of LLE model using SMC controller, the value of λ is selected as $diag[10 \quad 10 \quad 10 \quad 10 \quad 10]$. Selection of these values will result in equivalent control law similar to CTC in case 1. The constant k is selected as $[20 \quad 20 \quad 20 \quad 20 \quad 20]^T$ and the boundary layer thickness is taken as $\phi = [1 \quad 1 \quad 1 \quad 1 \quad 1]^T$.

Fig. 17 represents the stick diagram of one Gait cycle locomotion of LLE using SMC controller in presence of external disturbance torque. It can be seen clearly from the Fig 15 that SMC controller is able to track the desired swing leg trajectory and reject the external disturbance. The joint angle errors for this controller are shown in Fig. 18.

VI. CONCLUSION

The two-step locomotion of the dynamic model of a Lower Limb Exoskeleton is demonstrated via MATLAB simulations. The dynamic equation of motion of Exoskeleton system for the single support phase (SSP) is derived using the Euler - Lagrangian formulation.

The model validation is achieved by computer simulation using Computed torque controller and Sliding mode controller. The desired trajectories for full gait cycle are generated using time polynomial with constraints and inverse kinematic.

Since the effectiveness of computed torque control is directly related to the accuracy of the dynamic model. Any un-modeled dynamics, parametric uncertainty and external disturbance may lead to unacceptable performance. Another drawback of this control method arises due to the time required to compute the quantities $D(q)$, $C(\dot{q}, q)$ and $G(q)$. Conventional Sliding Mode Control method is able to reject the external disturbance. This method also ensures robustness to certain amount of uncertainty. However, implementation of this controller cause several issues. Chattering effect prevents the practical implementation of SMC. SMC with boundary layer suffers from the degradation of tracking performance and robustness. The future scope of this work includes the development of a robust/ adaptive control system for the lower limb exoskeleton to provide human locomotion augmentation, which can take care of un-modeled uncertainty of the system and external disturbances.

A suitable control system also increases the load-bearing capabilities while providing the augmentation. Classical control methods have been used in the control of the lower limb Exoskeletons/ Robotics system. However, most of the control methods are not robust to reject model uncertainties and disturbance, which leads to the risk of safety to the Exoskeleton's user, as these controllers may produce increasing power and torque in the presence of model uncertainty & disturbance. The use of a suitable robust/adaptive controller could guarantee the safety of the user.

ACKNOWLEDGMENT

We would like to convey our heartfelt gratitude to the Dr. R Indu Shekar, Scientist G, Director, DEBEL, and Dr. K Mohanavelu, Scientist G, Project Director - Exoskeleton, for providing the permission, guidance & infrastructure to carry out this research work.

REFERENCES

[1] T. McGeer, "Passive dynamic walking," *The International Journal of Robotics Research*, vol. 9, no. 2, pp. 62–82, 1990. [Online]. Available: https://doi.org/10.1177/027836499000900206 =0pt

[2] T. McGeer, "Passive walking with knees," in *Proceedings., IEEE International Conference on Robotics and Automation*, May 1990, pp. 1640–1645 vol.3.

[3] Xiuping Mu and Qiong Wu, "A complete dynamic model of five-link bipedal walking," in *Proceedings of the 2003 American Control Conference, 2003.*, vol. 6, June 2003, pp. 4926–4931 vol.6.

[4] "Dynamic modeling and sliding mode control of a five-link biped during the double support phase," in *Proceedings of the 2004 American Control Conference*, vol. 3, June 2004, pp. 2609–2614 vol.3.

[5] G. J. C. C. C. J. M. B. G. S. L. F. Westervelt, E., *Feedback Control of Dynamic Bipedal Robot Locomotion*. 1em plus 0.5em minus 0.4em Boca Raton: CRC Press, 2007.

[6] B. T. V. T. Moltedo, M., "Powered ankle-foot orthoses: the effects of the assistance on healthy and impaired users while walking," *Journal of NeuroEngineering and Rehabilitation* , vol. 15, no. 86, 2018.

[7] M. Spong, S. Hutchinson, and M. Vidyasagar, *Robot Modeling and Control*. 1em plus 0.5em minus 0.4em Wiley, 2005.

[8] M. O. Ajayi, "Modelling and control of actuated lower limb exoskeletons : a mathematical application using central pattern generators and nonlinear feedback control techniques," Ph.D. dissertation, UniversitÃ© Paris-Est, 2016.

[9] Y. Hurmuzlu, "Dynamics of Bipedal Gait: Part Iâ€"Objective Functions and the Contact Event of a Planar Five-Link Biped," *Journal of Applied Mechanics*, vol. 60, no. 2, pp. 331–336, 1993. [Online]. Available: https://doi.org/10.1115/1.2900797. =0pt

[10] S. Tzafestas, M. Raibert, and C. Tzafestas, "Robust sliding-mode control applied to a 5-link biped robot," *Journal of Intelligent and Robotic Systems*, vol. 15, pp. 67–133, 09 1996.

[11] X. Mu, "Dynamics and motion regulation of a five link biped robot walking in the sagittal pilane," Ph.D. dissertation, The University of Manitoba, 2004.

[12] K. Mitobe, N. Mori, Y. Nasu, and N. Adachi, "Control of a biped walking robot during the double support phase," *Autonomous Robots*, vol. 4, no. 3, pp. 287–296, Sep 1997. [Online]. Available: https://doi.org/10.1023/A:1008896010368 =0pt

[13] Qiang Huang, K. Yokoi, S. Kajita, K. Kaneko, H. Arai, N. Koyachi, and K. Tanie, "Planning walking patterns for a biped robot," *IEEE Transactions on Robotics and Automation*, vol. 17, no. 3, pp. 280–289, 2001.

[14] K. Mitobe, N. Mori, K. Aida, and Y. Nasu, "Nonlinear feedback control of a biped walking robot," in *Proceedings of 1995 IEEE International Conference on Robotics and Automation*, vol. 3, May 1995, pp. 2865–2870 vol.3.

[15] C. M. C. O. Valle, R. Tanscheit, and L. A. F. Mendoza, "Computed-torque control of a simulated bipedal robot with locomotion by reinforcement learning," in *2016 IEEE Latin American Conference on Computational Intelligence (LA-CCI)*, Nov 2016, pp. 1–6.

[16] J. Craig, *Introduction to Robotics: Mechanics and Control*, ser. Addison-Wesley series in electrical and computer engineering: control engineering. 1em plus 0.5em minus 0.4em Pearson/Prentice Hall, 2005.

[17] J.-J. E. Slotine and W. Li, "Applied nonlinear control," 1991.

[18] M. O. Ajayi, K. Djouani, and Y. Hamam, "Bounded control of a full-exoskeleton device with four (4) degree of freedom," in *2015 IEEE*

International Conference on Robotics and Biomimetics (ROBIO), Dec 2015, pp. 2425–2430.

[19] L. Sciavicco, B. Siciliano, and B. Sciavicco, *Modelling and Control of Robot Manipulators*, 2nd ed. 1em plus 0.5em minus 0.4em Berlin, Heidelberg: Springer-Verlag, 2000.

APPENDIX A
DERIVATION OF EQUATION OF MOTION

The Lagrangian is defined as

$$\mathcal{L} = K - P \tag{51}$$

Where $\mathcal{L}$ is Lagrangian, K is total Kinetic Energy of the system and P is total Potential Energy. The **Euler - Lagrange equation of motion** is given by eq. 52 [7].

$$\frac{d}{dt}\frac{\partial \mathcal{L}}{\partial \dot{q}_i} - \frac{\partial \mathcal{L}}{\partial q_i} = \tau_i \tag{52a}$$

$$\frac{d}{dt}\left(\frac{\partial K}{\partial \dot{q}_i}\right) - \frac{\partial K}{\partial q_i} + \frac{\partial P}{\partial q_i} = \tau_i \tag{52b}$$

Where q_i and τ_i represent the generalized coordinates and generalizes forces/ torques.

The general expression of kinetic and potential energy for n-link manipulator are discussed in the next sub-section

A. Computation of Kinetic Energy

The kinetic energy of the rigid body is sum of **translational energy** & **rotational kinetic energy**, and given as

$$K = \frac{1}{2}mv^T v + \frac{1}{2}\omega^T I\omega \tag{53}$$

Where m is the total mass of the object, v and ω are the linear and angular velocity vectors, respectively, and I is a symmetric 3×3 matrix called the Inertia Tensor [7].

The general expression for total kinetic energy of n link manipulator in terms of Jacobian matrix and the derivative of the joint variable is obtained by replacing the linear and angular velocities by $v_i = J_{v_i}(q)\dot{q}$ and $\omega_i = J_{\omega_i}(q)\dot{q}$ respectively.

$$\mathcal{K} = \frac{1}{2}\dot{q}^T \sum_{i=1}^{n} \left(m_i J_{v_i}(q)^T J_{v_i}(q) + J_{\omega_i}(q)^T I_i J_{\omega_i}(q)\right)\dot{q} \tag{54}$$

since, $\left(m_i J_{v_i}(q)^T J_{v_i}(q) + J_{\omega_i}(q)^T I_i J_{\omega_i}(q)\right) = D(q)$ is symmetric positive definite inertia matrix, equation (59) can be re-written in the following form [7]

$$\mathcal{K} = \frac{1}{2}\dot{q}^T D(q)\dot{q} \tag{55}$$

B. Computation of Potential Energy

For rigid body dynamics, only gravity contributes to the potential energy. Assuming the entire mass of the body to be concentrated at centre of mass, the potential energy of i^{th} link is given by

$$P_i = -g_o^T p_{c_i} m_i \tag{56}$$

where g_o is gravity acceleration vector in the base frame i.e. $g_o = [0,0,-g]'$ if z is vertical axis and p_{c_i} coordinates of the centre of mass of i^{th} link. therefore, the total energy of the n-link robot is

$$\mathcal{P} = -\sum_{i=1}^{n} P_i = -\sum_{i=1}^{n} g_o^T p_{c_i} m_i \tag{57}$$

The potential energy depends for the configuration of robot not on its velocity.

C. Equation of Motion

The Lagrangian, $\mathcal{L}(q,\dot{q}) = \mathcal{K}(q,\dot{q}) - \mathcal{P}(q)$, using (55) and (57), is given by

$$\mathcal{L} = \frac{1}{2}\sum_{i=1}^{n}\sum_{j=1}^{n} d_{ij}(q)\dot{q}_i\dot{q}_j - \mathcal{P}(q) \tag{58}$$

By substituting the (58) in (52), we get

$$\begin{aligned}\frac{d}{dt}\left(\frac{\partial \mathcal{L}}{\partial \dot{q}_i}\right) &= \frac{d}{dt}\left(\frac{\partial \mathcal{K}}{\partial \dot{q}_i}\right) = \sum_{j=1}^{n} d_{ij}(q)\ddot{q}_j + \sum_{j=1}^{n} \frac{d}{dt} d_{ij}(q)\dot{q}_j \\ &= \sum_{j=1}^{n} d_{ij}(q)\ddot{q}_i + \sum_{j=1}^{n}\sum_{k=1}^{n} \frac{\partial d_{ij}(q)}{\partial q_k}\dot{q}_k\dot{q}_j\end{aligned} \tag{59}$$

and also

$$\frac{\partial \mathcal{K}}{\partial q_i} = \frac{1}{2}\sum_{j,k}^{n} \frac{\partial d_{ik}(q)}{\partial q_i}\dot{q}_k\dot{q}_j \tag{60}$$

further

$$\frac{\partial \mathcal{P}}{\partial q_i} = -\sum_{j=1}^{n}\left(m_i g_o^T \frac{\partial p_{c_i}}{\partial q_i}\right) = -\sum_{j=1}^{n}\left(m_i g_o^T J_{pc}^i(q)\right) = g_i(q) \tag{61}$$

As a result, the equation of motion is obtained by combining above three equations

$$\sum_{j=1}^{n} d_{ij}(q)\ddot{q}_j + \sum_{j=1}^{n}\sum_{k=1}^{n} h_{ijk}(q)\dot{q}_k\dot{q}_j + g_i(q) = \tau_i \tag{62}$$

where $h_{ijk} = \frac{\partial d_{ij}(q)}{\partial q_k} - \frac{1}{2}\frac{\partial d_{ik}(q)}{\partial q_i}$.

Equation (67) in matrix form is represented by (1).

Where C is a suitable $n \times n$ matrix such that its elements C_{ij} satisfy the following equation [19].

$$\sum_{j=1}^{n} C_{ij}\dot{q}_j = \sum_{j=1}^{n}\sum_{k=1}^{n} h_{ijk}(q)\dot{q}_k\dot{q}_j \tag{63}$$

The generic element of C is given as

$$C_{ij} = \sum_{k=1}^{n} C_{ijk}\dot{q}_k \tag{64}$$

where the coefficients *(christiffel symbols of the first type)* are given as

$$C_{ijk} = \frac{1}{2}\left(\frac{\partial d_{ij}}{\partial q_k} + \frac{\partial d_{ik}}{\partial q_j} - \frac{\partial d_{jk}}{\partial q_i}\right) \tag{65}$$

Since the matrix D is symmetric, then $C_{ijk} = C_{ikj}$.

APPENDIX B
DYNAMIC MODEL OF FIVE LINK BIPED

After deriving the expression for total kinetic energy, Elements of Inertia matrix for biped model can be determined using (55). The elements of inertia matrix are given in (70) to (74). Similarly, The elements of Coriolis / centrifugal matrix are derived using (64) & (69). The elements of Coriolis/centrifugal matrix are given in (75) to (79).

Kinetic energy of COM of each link as per equation (53) is represented as

$$k_1 = \frac{1}{2}\dot{\theta}_1^{\,2}\left(m_1 d_1^{\,2} + I_1\right) \tag{66a}$$

$$\begin{aligned} k_2 &= \frac{1}{2}m_2 L_1^{\,2}\dot{\theta}_1^{\,2} + m_2\cos(\theta_1-\theta_2)L_1 d_2\dot{\theta}_1\dot{\theta}_2 \\ &+\frac{1}{2}m_2 d_2^{\,2}\dot{\theta}_2^{\,2} + \frac{1}{2}I_2\dot{\theta}_2^{\,2} \end{aligned} \tag{66b}$$

$$\begin{aligned} k_3 &= \frac{1}{2}m_3 L_1^{\,2}\dot{\theta}_1^{\,2} + m_3\cos(\theta_1-\theta_2)L_1 L_2\dot{\theta}_1\dot{\theta}_2 \\ &+m_3\cos(\theta_1-\theta_3)L_1 d_3\dot{\theta}_1\dot{\theta}_3 + \frac{1}{2}m_3 L_2^{\,2}\dot{\theta}_2^{\,2} \\ &+m_3\cos(\theta_2-\theta_3)L_2 d_3\dot{\theta}_2\dot{\theta}_3 + \frac{1}{2}\dot{\theta}_3^{\,2}\left(m_3 d_3^{\,2} + I_3\right) \end{aligned} \tag{66c}$$

$$\begin{aligned} k_4 &= \frac{1}{2}m_4 L_1^{\,2}\dot{\theta}_1^{\,2} + m_4\cos(\theta_1-\theta_2)L_1 L_2\dot{\theta}_1\dot{\theta}_2 \\ &+m_4\cos(\theta_1+\theta_4)L_1 L_4\dot{\theta}_1\dot{\theta}_4 + \frac{1}{2}m_4 d_4^{\,2}\dot{\theta}_4^{\,2} \\ &-m_4\cos(\theta_1+\theta_4)L_1 d_4\dot{\theta}_1\dot{\theta}_4 - m_4 L_4 d_4\dot{\theta}_4^{\,2} \\ &+\frac{1}{2}m_4 L_2^{\,2}\dot{\theta}_2^{\,2} + m_4\cos(\theta_2+\theta_4)L_2 L_4\dot{\theta}_2\dot{\theta}_4 \\ &-m_4\cos(\theta_2+\theta_4)L_2 d_4\dot{\theta}_2\dot{\theta}_4 + \frac{1}{2}\dot{\theta}_4^{\,2}(m_4 L_4^{\,2} + I_4) \end{aligned} \tag{66d}$$

$$\begin{aligned} k_5 &= \frac{1}{2}m_5\left\{L_1^{\,2}\dot{\theta}_1^{\,2} + L_2^{\,2}\dot{\theta}_2^{\,2} + L_4^{\,2}\dot{\theta}_4^{\,2} + L_5^{\,2}\dot{\theta}_5^{\,2}\right. \\ &\left.+d_5^{\,2}\dot{\theta}_5^{\,2}\right\} + m_5\cos(\theta_1-\theta_2)L_1 L_2\dot{\theta}_1\dot{\theta}_2 \\ &+m_5\cos(\theta_1+\theta_4)L_1 L_4\dot{\theta}_1\dot{\theta}_4 + \frac{1}{2}I_5\dot{\theta}_5^{\,2} \\ &+m_5\cos(\theta_1+\theta_5)L_1 L_5\dot{\theta}_1\dot{\theta}_5\{L_5-d_5\} \\ &+m_5\cos(\theta_2+\theta_4)L_2 L_4\dot{\theta}_2\dot{\theta}_4 - m_5 L_5 d_5\dot{\theta}_5^{\,2} \\ &+m_5\cos(\theta_2+\theta_5)L_2 L_5\dot{\theta}_2\dot{\theta}_5\{L_5-d_5\} \\ &+m_5\cos(\theta_4-\theta_5)L_4\dot{\theta}_4\dot{\theta}_5\{L_5-d_5\} \end{aligned} \tag{66e}$$

Potential energy of COM of each link as per Eq. (61)

$$\begin{aligned} p_1 &= d_1 g m_1\cos(\theta_1) \\ p_2 &= g m_2\left(L_1\cos(\theta_1) + d_2\cos(\theta_2)\right) \\ p_3 &= g m_3\left(L_1\cos(\theta_1) + L_2\cos(\theta_2) + d_3\cos(\theta_3)\right) \\ p_4 &= g m_4\left(L_1\cos(\theta_1) + L_2\cos(\theta_2)\right. \\ &\left.-\cos(\theta_4)(L_4-d_4)\right) \\ p_5 &= g m_5\left(L_1\cos(\theta_1) + L_2\cos(\theta_2) - L_4\cos(\theta_4)\right. \\ &\left.-\cos(\theta_5)(L_5-d_5)\right) \end{aligned} \tag{67}$$

Total Kinetic Energy $\mathcal{K} = k_1 + k_2 + k_3 + k_4 + k_5$ of system is given by Eq. (77.) Similarly, the total Potential energy $\mathcal{P} = p_1 + p_2 + p_3 + p_4 + p_5$ of system is given by Eq. (78).

Total Kinetic Energy

$$\begin{aligned} \mathcal{K} &= \frac{1}{2}\left(I_1\dot{\theta}_1^{\,2} + I_2\dot{\theta}_2^{\,2} + I_3\dot{\theta}_3^{\,2} + I_4\dot{\theta}_4^{\,2} + I_5\dot{\theta}_5^{\,2}\right) \\ &-L_4 d_4 m_4\dot{\theta}_4^{\,2} + \frac{1}{2}L_1^{\,2}\dot{\theta}_1^{\,2}(m_2+m_3+m_4+m_5) \\ &+\frac{1}{2}L_4^{\,2}\dot{\theta}_4^{\,2}(m_4+m_5) + \frac{1}{2}L_2^{\,2}\dot{\theta}_2^{\,2}(m_3+m_4+m_5) \\ &+L_1 d_3 m_3\dot{\theta}_1\dot{\theta}_3\cos(\theta_1-\theta_3) + \frac{1}{2}d_1^{\,2}m_1\dot{\theta}_1^{\,2} \\ &+L_2 d_3 m_3\dot{\theta}_2\dot{\theta}_3\cos(\theta_2-\theta_3) + \frac{1}{2}\left(L_5^{\,2} + d_5^{\,2}\right)m_5\dot{\theta}_5^{\,2} \\ &+\frac{1}{2}d_2^{\,2}m_2\dot{\theta}_2^{\,2} + \frac{1}{2}d_3^{\,2}m_3\dot{\theta}_3^{\,2} + \frac{1}{2}d_4^{\,2}m_4\dot{\theta}_4^{\,2} \\ &-L_5 d_5 m_5\dot{\theta}_5^{\,2} + L_1 d_2 m_2\dot{\theta}_1\dot{\theta}_2\cos(\theta_1-\theta_2) \\ &+L_1(L_5-d_5)m_5\dot{\theta}_1\dot{\theta}_5\cos(\theta_1+\theta_5) \\ &+L_2(L_5-d_5)m_5\dot{\theta}_2\dot{\theta}_5\cos(\theta_2+\theta_5) \\ &+L_1 L_2(m_3+m_4+m_5)\dot{\theta}_1\dot{\theta}_2\cos(\theta_1-\theta_2) \\ &+L_4(L_5-d_5)m_5\dot{\theta}_4\dot{\theta}_5\cos(\theta_4-\theta_5) \\ &+L_1(L_4 m_4 + L_4 m_5 - d_4 m_4)\dot{\theta}_1\dot{\theta}_4\cos(\theta_1+\theta_4) \\ &+L_2(L_4 m_4 + L_4 m_5 - d_4 m_4)\dot{\theta}_2\dot{\theta}_4\cos(\theta_2+\theta_4) \end{aligned} \tag{68}$$

Total Potential Energy

$$\begin{aligned} \mathcal{P} &= g m_5\{L_1\cos(\theta_1) + L_2\cos(\theta_2) - L_4\cos(\theta_4) \\ &-L_5\cos(\theta_5) + d_5\cos(\theta_5)\} + g m_3\{L_1\cos(\theta_1) \\ &+L_2\cos(\theta_2) + d_3\cos(\theta_3)\} + g m_4\{L_1\cos(\theta_1) \\ &+L_2\cos(\theta_2) - L_4\cos(\theta_4) + d_4\cos(\theta_4)\} \\ &+g m_2\{L_1\cos(\theta_1) + d_2\cos(\theta_2)\} + g m_1 d_1\cos(\theta_1) \end{aligned} \tag{69}$$

Inertia Matrix Elements

$$\begin{aligned} D_{11} &= I_1 + L_1^{\,2}(m_2+m_3+m_4+m_5) + d_1^{\,2}m_1 \\ D_{12} &= L_1\cos(\theta_1-\theta_2)(L_2(m_3+m_4+m_5) + d_2 m_2) \\ D_{13} &= L_1 d_3 m_3\cos(\theta_1-\theta_3) \\ D_{14} &= L_1\cos(\theta_1+\theta_4)(L_4 m_4 + L_4 m_5 - d_4 m_4) \\ D_{15} &= L_1 m_5\cos(\theta_1+\theta_5)(L_5-d_5) \end{aligned} \tag{70}$$

$$\begin{aligned} D_{21} &= D_{12} \\ D_{22} &= I_2 + L_2^{\,2}(m_3+m_4+m_5) + d_2^{\,2}\,m_2 \\ D_{23} &= L_2\,d_3\,m_3\,\cos(\theta_2-\theta_3) \\ D_{24} &= L_2\,\cos(\theta_2+\theta_4)\,(L_4\,m_4 + L_4\,m_5 - d_4\,m_4) \\ D_{25} &= L_2\,m_5\,\cos(\theta_2+\theta_5)\,(L_5-d_5) \end{aligned} \tag{71}$$

$$\begin{aligned} D_{31} &= D_{13},\quad D_{32} = D_{23} \\ D_{33} &= m_3 d_3^{\,2} + I_3,\quad D_{34} = D_{35} = 0 \end{aligned} \tag{72}$$

$$\begin{aligned} D_{41} &= D_{14},\quad D_{42} = D_{24},\quad D_{43} = 0 \\ D_{44} &= I_4 + L_4^{\,2}\,m_4 + L_4^{\,2}\,m_5 + d_4^{\,2}\,m_4 - 2\,L_4\,d_4\,m_4 \\ D_{45} &= L_4\,m_5\,\cos(\theta_4-\theta_5)\,(L_5-d_5) \end{aligned} \tag{73}$$

$$\begin{aligned} D_{51} &= D_{15},\quad D_{52} = D_{25}\quad D_{53} = 0 \\ D_{54} &= D_{45} \\ D_{55} &= m_5\,L_5^{\,2} - 2\,m_5\,L_5\,d_5 + m_5\,d_5^{\,2} + I_5 \end{aligned} \tag{74}$$

Coriolis/centrifugal Matrix Elements

$$\begin{aligned}
C_{11} &= 0 \\
C_{12} &= L_1\dot{\theta}_2\sin(\theta_1-\theta_2)(L_2(m_3+m_4+m_5)+d_2m_2) \\
C_{13} &= L_1\, d_3\, m_3\, \dot{\theta}_3 \sin(\theta_1-\theta_3) \\
C_{14} &= -L_1\dot{\theta}_4\sin(\theta_1+\theta_4)(L_4(m_4+m_5)-d_4\, m_4) \\
C_{15} &= -L_1\, m_5\, \dot{\theta}_5 \sin(\theta_1+\theta_5)\,(L_5-d_5)
\end{aligned} \tag{75}$$

$$\begin{aligned}
C_{21} &= -L_1\, \dot{\theta}_1 \sin(\theta_1-\theta_2)\,(L_2(m_3+m_4+m_5)+d_2\, m_2) \\
C_{22} &= 0, C_{23} = L_2\, d_3\, m_3\, \dot{\theta}_3 \sin(\theta_2-\theta_3) \\
C_{24} &= -L_2\, \dot{\theta}_4 \sin(\theta_2+\theta_4)\,(L_4\, m_4+L_4\, m_5-d_4\, m_4) \\
C_{25} &= -L_2\, m_5\, \dot{\theta}_5 \sin(\theta_2+\theta_5)\,(L_5-d_5)
\end{aligned} \tag{76}$$

$$\begin{aligned}
C_{31} &= -L_1\, d_3\, m_3\, \dot{\theta}_1\sin(\theta_1-\theta_3) \\
C_{32} &= -L_2\, d_3\, m_3\, \dot{\theta}_2 \sin(\theta_2-\theta_3) \\
C_{33} &= 0, \quad C_{34} = 0, \quad C_{35} = 0
\end{aligned} \tag{77}$$

$$\begin{aligned}
C_{41} &= -L_1\, \dot{\theta}_1 \sin(\theta_1+\theta_4)\,(L_4\, m_4+L_4\, m_5-d_4\, m_4) \\
C_{42} &= -L_2\, \dot{\theta}_2 \sin(\theta_2+\theta_4)\,(L_4\, m_4+L_4\, m_5-d_4\, m_4) \\
C_{43} &= 0, \quad C_{44} = 0 \\
C_{45} &= L_4\, m_5\, \dot{\theta}_5 \sin(\theta_4-\theta_5)\,(L_5-d_5)
\end{aligned} \tag{78}$$

$$\begin{aligned}
C_{51} &= -L_1\, m_5\, \dot{\theta}_1 \sin(\theta_1+\theta_5)\,(L_5-d_5) \\
C_{52} &= -L_2\, m_5\, \dot{\theta}_2 \sin(\theta_2+\theta_5)\,(L_5-d_5) \\
C_{53} &= 0, \quad C_{54} = -L_4\, m_5\, \dot{\theta}_4 \sin(\theta_4-\theta_5)\,(L_5-d_5) \\
C_{55} &= 0
\end{aligned} \tag{79}$$

Gravitational Torque Elements

$$\begin{aligned}
G_1 &= -g\sin(\theta_1)\{L_1(m_2+m_3+m_4+L_1m_5)+d_1m_1\} \\
G_2 &= -g\sin(\theta_2)\{L_2(m_3+m_4+m_5)+d_2m_2\} \\
G_3 &= -d_3\, g\, m_3 \sin(\theta_3) \\
G_4 &= g\sin(\theta_4)\,(L_4\, m_4+L_4\, m_5-d_4\, m_4) \\
G_5 &= g\, m_5 \sin(\theta_5)\,(L_5-d_5)
\end{aligned} \tag{80}$$

Appendix C

Dynamic Model of Five Link Biped in term of relative joints variables

Inertia Matrix Elements

$$\begin{aligned}
D_{q_{11}} &= I_1+I_2+I_3+I_4+I_5+L_1{}^2m_2+L_1{}^2m_3+L_1{}^2m_4 \\
&+L_2{}^2m_3+L_1{}^2m_5+L_2{}^2m_4+L_2{}^2m_5+L_4{}^2m_4+L_4{}^2m_5 \\
&+L_5{}^2m_5+d_1{}^2m_1+d_2{}^2m_2+d_3{}^2m_3+d_4{}^2m_4+d_5{}^2m_5 \\
&-2L_2\cos(q_2+q_3)(L_4m_4+L_4m_5-d_4m_4)+2L_1\cos(q_1) \\
&*(L_2m_3+L_2m_4+L_2m_5+d_2m_2)-2L_4d_4m_4 \\
&-2L_5d_5m_5-2L_1\cos(q_1+q_2+q_3)(L_4m_4+L_4m_5 \\
&-d_4m_4)+2L_1d_3m_3\cos(q_1+q_2)+2L_2d_3m_3\cos(q_2) \\
&+2L_4m_5\cos(q_4)(L_5-d_5)-2L_1m_5\cos(q_1+q_2+q_3 \\
&-q_4)(L_5-d_5)-2L_2m_5\cos(q_2+q_3-q_4)(L_5-d_5)
\end{aligned}$$

$$\begin{aligned}
D_{q_{12}} &= 2L_2\cos(q_2+q_3)(L_4m_4+L_4m_5-d_4m_4)-I_3-I_4-I_5 \\
&-L_2{}^2m_3-L_2{}^2m_4-L_2{}^2m_5-L_4{}^2m_4-L_4{}^2m_5-L_5{}^2m_5 \\
&-d_2{}^2m_2-d_3{}^2m_3-d_4{}^2m_4-d_5{}^2m_5-I_2-L_1\cos(q_1) \\
&*(L_2m_3+L_2m_4+L_2m_5+d_2m_2)+2L_4d_4m_4+2L_5d_5m_5 \\
&+L_1\cos(q_1+q_2+q_3)(L_4m_4+L_4m_5-d_4m_4) \\
&-L_1d_3m_3\cos(q_1+q_2)-2L_2d_3m_3\cos(q_2) \\
&-2L_4m_5\cos(q_4)(L_5-d_5)+m_5(L_5-d_5)(L_1\cos(q_1+q_2 \\
&+q_3-q_4)+2L_2\cos(q_2+q_3-q_4))
\end{aligned}$$

$$\begin{aligned}
D_{q_{13}} &= L_2\cos(q_2+q_3)(L_4m_4+L_4m_5-d_4m_4)-I_4-I_5 \\
&-L_4{}^2m_4-L_4{}^2m_5-L_5{}^2m_5-d_3{}^2m_3-d_4{}^2m_4-d_5{}^2m_5 \\
&-I_3+2L_4d_4m_4+2L_5d_5m_5+L_1\cos(q_1+q_2+q_3)(L_4m_4 \\
&+L_4m_5-d_4m_4)-L_1d_3m_3\cos(q_1+q_2)-L_2d_3m_3\cos(q_2) \\
&-2L_4m_5\cos(q_4)(L_5-d_5)+L_1m_5\cos(q_1+q_2+q_3-q_4) \\
&*(L_5-d_5)+L_2m_5\cos(q_2+q_3-q_4)(L_5-d_5)
\end{aligned}$$

$$\begin{aligned}
D_{1_{14}} &= L_2\cos(q_2+q_3)(L_4m_4+L_4m_5-d_4m_4)-I_5-L_4{}^2m_4 \\
&-L_4{}^2m_5-L_5{}^2m_5-d_4{}^2m_4-d_5{}^2m_5-I_4+2L_4d_4m_4 \\
&+2L_5d_5m_5+L_1\cos(q_1+q_2+q_3)(L_4m_4+L_4m_5-d_4m_4) \\
&-2L_4m_5\cos(q_4)(L_5-d_5)+m_5(L_5-d_5)(L_1\cos(q_1+q_2 \\
&+q_3-q_4)+L_2\cos(q_2+q_3-q_4))
\end{aligned}$$

$$\begin{aligned}
D_{q_{15}} &= I_5+L_5{}^2m_5+d_5{}^2m_5-2L_5d_5m_5 \\
&+L_4m_5\cos(q_4)(L_5-d_5)-m_5(L_5-d_5)(L_1\cos(q_1+q_2 \\
&+q_3-q_4)+L_2m_5\cos(q_2+q_3-q_4)) \\
D_{q_{21}} &= D_{q_{12}}
\end{aligned}$$

$$\begin{aligned}
D_{q_{22}} &= I_2+I_3+I_4+I_5+L_2{}^2m_3+L_2{}^2m_4+L_2{}^2m_5+L_4{}^2m_4 \\
&+L_4{}^2m_5+L_5{}^2m_5+d_2{}^2m_2+d_3{}^2m_3+d_4{}^2m_4+d_5{}^2m_5 \\
&-2L_2\cos(q_2+q_3)(L_4m_4+L_4m_5-d_4m_4)-2L_4d_4m_4 \\
&-2L_5d_5m_5+2L_2d_3m_3\cos(q_2)+2L_4m_5\cos(q_4)(L_5-d_5) \\
&-2L_2m_5\cos(q_2+q_3-q_4)(L_5-d_5)
\end{aligned}$$

$$\begin{aligned}
D_{q_{23}} &= I_3+I_4+I_5+L_4{}^2m_4+L_4{}^2m_5+L_5{}^2m_5+d_3{}^2m_3 \\
&+d_4{}^2m_4+d_5{}^2m_5-L_2\cos(q_2+q_3)(L_4m_4+L_4m_5 \\
&-d_4m_4)-2L_4d_4m_4-2L_5d_5m_5+L_2d_3m_3\cos(q_2) \\
&+m_5(L_5-d_5)\big(2L_4\cos(q_4)-L_2\cos(q_2+q_3-q_4)\big)
\end{aligned}$$

$$\begin{aligned}
D_{q_{24}} &= I_4+I_5+L_4{}^2m_4+L_4{}^2m_5+L_5{}^2m_5+d_4{}^2m_4+d_5{}^2m_5 \\
&-L_2\cos(q_2+q_3)(L_4m_4+L_4m_5-d_4m_4)-2L_4d_4m_4 \\
&-2L_5d_5m_5+2L_4m_5\cos(q_4)(L_5-d_5) \\
&-L_2m_5\cos(q_2+q_3-q_4)(L_5-d_5)
\end{aligned}$$

$$\begin{aligned}
D_{q_{25}} &= 2L_5d_5m_5-L_5{}^2m_5-d_5{}^2m_5-I_5-L_4m_5\cos(q_4) \\
&*(L_5-d_5)+L_2m_5\cos(q_2+q_3-q_4)(L_5-d_5) \\
D_{q_{31}} &= D_{q_{13}}, \quad D_{q_{32}} = D_{q_{23}}
\end{aligned}$$

$$D_{q33} = I_3 + I_4 + I_5 + {L_4}^2 m_4 + {L_4}^2 m_5 + {L_5}^2 m_5 + {d_3}^2 m_3 + {d_4}^2 m_4 + {d_5}^2 m_5 - 2L_4 d_4 m_4 - 2L_5 d_5 m_5 + 2L_4 m_5 \cos(q_4)(L_5 - d_5)$$

$$D_{q_{34}} = I_4 + I_5 + {L_4}^2 m_4 + {L_4}^2 m_5 + {L_5}^2 m_5 + {d_4}^2 m_4 + {d_5}^2 m_5 - 2L_4 d_4 m_4 - 2L_5 d_5 m_5 + 2L_4 m_5 \cos(q_4)(L_5 - d_5)$$

$$D_{q_{35}} = 2L_5 d_5 m_5 - {L_5}^2 m_5 - {d_5}^2 m_5 - I_5 - L_4 m_5 \cos(q_4)(L_5 - d_5)$$

$$D_{q_{41}} = D_{q_{14}} \quad D_{q_{42}} = D_{q_{24}}$$

$$D_{q_{43}} = D_{q_{44}} = D_{q_{34}}, \quad D_{q_{45}} = D_{q_{35}}$$

$$D_{q_{51}} = D_{q_{15}}, \quad D_{q_{52}} = D_{q_{25}}, \quad D_{q_{53}} = D_{q_{54}} = D_{q_{35}}$$

$$D_{q_{55}} = m_5\, {L_5}^2 - 2\, m_5\, L_5\, d_5 + m_5\, {d_5}^2 + I_5$$

Coriolis/centrifugal Matrix Elements

$$C_{q_{11}} = L_1 \dot{q}_0 \sin(q_1 + q_2 + q_3)(L_4 m_4 + L_4 m_5 - d_4 m_4) + L_1 \sin(q_1)(\dot{q}_0 - \dot{q}_1)(L_2 m_3 + L_2 m_4 + L_2 m_5 + d_2 m_2) + L_1 \sin(q_1 + q_2 + q_3)(L_4 m_4 + L_4 m_5 - d_4 m_4)(\dot{q}_1 - \dot{q}_0 + \dot{q}_2 + \dot{q}_3) + L_2 \sin(q_2 + q_3)(L_4 m_4 + L_4 m_5 - d_4 m_4)(\dot{q}_1 - \dot{q}_0 + \dot{q}_2 + \dot{q}_3) + L_2 \sin(q_2 + q_3)(\dot{q}_0 - \dot{q}_1)(L_4 m_4 + L_4 m_5 - d_4 m_4) - L_1 \dot{q}_0 \sin(q_1)(L_2 m_3 + L_2 m_4 + L_2 m_5 + d_2 m_2) - L_2 d_3 m_3 \sin(q_2)(\dot{q}_0 - \dot{q}_1) - L_1 d_3 m_3 \sin(q_1 + q_2)(\dot{q}_1 - \dot{q}_0 + \dot{q}_2) + L_2 m_5 \sin(q_2 + q_3 - q_4)(L_5 - d_5)(\dot{q}_1 - \dot{q}_0 + \dot{q}_2 + \dot{q}_3 - \dot{q}_4) - L_2 d_3 m_3 \sin(q_2)(\dot{q}_1 - \dot{q}_0 + \dot{q}_2) - L_1 d_3 m_3 \dot{q}_0 * \sin(q_1 + q_2) + L_2 m_5 \sin(q_2 + q_3 - q_4)(L_5 - d_5)(\dot{q}_0 - \dot{q}_1) + m_5 (L_5 - d_5)(\dot{q}_1 - \dot{q}_0 + \dot{q}_2 + \dot{q}_3 - \dot{q}_4)(L_4 \sin(q_4) + L_1 \sin(q_1 + q_2 + q_3 - q_4)\big) + m_5 (L_5 - d_5)(L_1 \dot{q}_0 \sin(q_1 + q_2 + q_3 - q_4) - L_4 \sin(q_4)(\dot{q}_1 - \dot{q}_0 + \dot{q}_2 + \dot{q}_3)\big)$$

$$C_{q_{12}} = L_2 d_3 m_3 \sin(q_2)(\dot{q}_0 - \dot{q}_1) - L_1 \sin(q_1 + q_2 + q_3)(L_4 m_4 + L_4 m_5 - d_4 m_4)(\dot{q}_1 - \dot{q}_0 + \dot{q}_2 + \dot{q}_3) - L_2 \sin(q_2 + q_3) * (L_4 m_4 + L_4 m_5 - d_4 m_4)(\dot{q}_1 - \dot{q}_0 + \dot{q}_2 + \dot{q}_3) - L_2 \sin(q_2 + q_3)(\dot{q}_0 - \dot{q}_1)(L_4 m_4 + L_4 m_5 - d_4 m_4) - L_1 \sin(q_1)(\dot{q}_0 - \dot{q}_1)(L_2 m_3 + L_2 m_4 + L_2 m_5 + d_2 m_2) + L_1 d_3 m_3 \sin(q_1 + q_2)(\dot{q}_1 - \dot{q}_0 + \dot{q}_2) - L_2 m_5 \sin(q_2 + q_3 - q_4)(L_5 - d_5) * (\dot{q}_1 - \dot{q}_0 + \dot{q}_2 + \dot{q}_3 - \dot{q}_4) + L_2 d_3 m_3 \sin(q_2)(\dot{q}_1 - \dot{q}_0 + \dot{q}_2) - L_2 m_5 \sin(q_2 + q_3 - q_4)(L_5 - d_5)(\dot{q}_0 - \dot{q}_1) - L_4 m_5 \sin(q_4)(L_5 - d_5)(\dot{q}_1 - \dot{q}_0 + \dot{q}_2 + \dot{q}_3 - \dot{q}_4) - L_1 m_5 \sin(q_1 + q_2 + q_3 - q_4)(L_5 - d_5)(\dot{q}_1 - \dot{q}_0 + \dot{q}_2 + \dot{q}_3 - \dot{q}_4) + L_4 m_5 \sin(q_4)(L_5 - d_5)(\dot{q}_1 - \dot{q}_0 + \dot{q}_2 + \dot{q}_3)$$

$$C_{q_{13}} = L_1 d_3 m_3 \sin(q_1 + q_2)(\dot{q}_1 - \dot{q}_0 + \dot{q}_2) - L_2 \sin(q_2 + q_3) * (L_4 m_4 + L_4 m_5 - d_4 m_4)(\dot{q}_1 - \dot{q}_0 + \dot{q}_2 + \dot{q}_3) - L_1 \sin(q_1 + q_2 + q_3)(L_4 m_4 + L_4 m_5 - d_4 m_4)(\dot{q}_1 - \dot{q}_0 + \dot{q}_2 + \dot{q}_3) - L_2 m_5 \sin(q_2 + q_3 - q_4)(L_5 - d_5)(\dot{q}_1 + \dot{q}_2 + \dot{q}_3 - \dot{q}_4) + L_2 d_3 m_3 \sin(q_2)(\dot{q}_1 - \dot{q}_0 + \dot{q}_2) - L_4 m_5 \sin(q_4)(L_5 - d_5) * (\dot{q}_1 - \dot{q}_0 + \dot{q}_2 + \dot{q}_3 - \dot{q}_4) - L_1 m_5 \sin(q_1 + q_2 + q_3 - q_4) * (L_5 - d_5)(\dot{q}_1 - \dot{q}_0 + \dot{q}_2 + \dot{q}_3 - \dot{q}_4) + L_4 m_5 \sin(q_4)(L_5 - d_5)(\dot{q}_1 - \dot{q}_0 + \dot{q}_2 + \dot{q}_3)$$

$$C_{q_{14}} = L_4 m_5 \sin(q_4)(L_5 - d_5)(\dot{q}_1 - \dot{q}_0 + \dot{q}_2 + \dot{q}_3) - L_2 \sin(q_2 + q_3)(L_4 m_4 + L_4 m_5 - d_4 m_4)(\dot{q}_1 - \dot{q}_0 + \dot{q}_2 + \dot{q}_3) - m_5 (L_5 - d_5)(\dot{q}_1 - \dot{q}_0 + \dot{q}_2 + \dot{q}_3 - \dot{q}_4)\{L_2 \sin(q_2 + q_3 - q_4) + L_4 \sin(q_4) + L_1 \sin(q_1 + q_2 + q_3 - q_4)\} - L_1 \sin(q_1 + q_2 + q_3)(L_4 m_4 + L_4 m_5 - d_4 m_4) * (\dot{q}_1 - \dot{q}_0 + \dot{q}_2 + \dot{q}_3)$$

$$C_{q_{15}} = L_2 m_5 \sin(q_2 + q_3 - q_4)(L_5 - d_5)(\dot{q}_1 - \dot{q}_0 + \dot{q}_2 + \dot{q}_3 - \dot{q}_4) + L_4 m_5 \sin(q_4)(L_5 - d_5)(\dot{q}_1 - \dot{q}_0 + \dot{q}_2 + \dot{q}_3 - \dot{q}_4) + L_1 m_5 \sin(q_1 + q_2 + q_3 - q_4)(L_5 - d_5) * (\dot{q}_1 - \dot{q}_0 + \dot{q}_2 + \dot{q}_3 - \dot{q}_4)$$

$$C_{q_{21}} = L_1 \dot{q}_0 \sin(q_1)(L_2 m_3 + L_2 m_4 + L_2 m_5 + d_2 m_2) - L_2 \sin(q_2 + q_3)(L_4 m_4 + L_4 m_5 - d_4 m_4)(\dot{q}_1 - \dot{q}_0 + \dot{q}_2 + \dot{q}_3) - L_2 \sin(q_2 + q_3)(\dot{q}_0 - \dot{q}_1)(L_4 m_4 + L_4 m_5 - d_4 m_4) - L_1 \dot{q}_0 \sin(q_1 + q_2 + q_3)(L_4 m_4 + L_4 m_5 - d_4 m_4) + L_2 d_3 m_3 \sin(q_2)(\dot{q}_0 - \dot{q}_1) - L_2 m_5 \sin(q_2 + q_3 - q_4)(L_5 - d_5)(\dot{q}_1 - \dot{q}_0 + \dot{q}_2 + \dot{q}_3 - \dot{q}_4) + L_2 d_3 m_3 \sin(q_2)(\dot{q}_1 - \dot{q}_0 + \dot{q}_2) + L_1 d_3 m_3 \dot{q}_0 \sin(q_1 + q_2) - L_2 m_5 \sin(q_2 + q_3 - q_4) * (L_5 - d_5)(\dot{q}_0 - \dot{q}_1) - L_4 m_5 \sin(q_4)(L_5 - d_5)(\dot{q}_1 - \dot{q}_0 + \dot{q}_2 + \dot{q}_3 - \dot{q}_4) - L_1 m_5 \dot{q}_0 \sin(q_1 + q_2 + q_3 - q_4)(L_5 - d_5) + L_4 m_5 \sin(q_4)(L_5 - d_5)(\dot{q}_1 - \dot{q}_0 + \dot{q}_2 + \dot{q}_3)$$

$$C_{q_{22}} = L_2 \sin(q_2 + q_3)(L_4 m_4 + L_4 m_5 - d_4 m_4)(\dot{q}_1 - \dot{q}_0 + \dot{q}_2 + \dot{q}_3) + L_2 \sin(q_2 + q_3)(\dot{q}_0 - \dot{q}_1)(L_4 m_4 + L_4 m_5 - d_4 m_4) - L_2 d_3 m_3 \sin(q_2)(\dot{q}_0 - \dot{q}_1) + L_2 m_5 \sin(q_2 + q_3 - q_4)(L_5 - d_5)(\dot{q}_1 - \dot{q}_0 + \dot{q}_2 + \dot{q}_3 - \dot{q}_4) - L_2 d_3 m_3 \sin(q_2)(\dot{q}_1 - \dot{q}_0 + \dot{q}_2) + L_2 m_5 \sin(q_2 + q_3 - q_4)(L_5 - d_5)(\dot{q}_0 - \dot{q}_1) + L_4 m_5 \sin(q_4)(L_5 - d_5)(\dot{q}_1 - \dot{q}_0 + \dot{q}_2 + \dot{q}_3 - \dot{q}_4) - L_4 m_5 \sin(q_4)(L_5 - d_5)(\dot{q}_1 - \dot{q}_0 + \dot{q}_2 + \dot{q}_3)$$

$$C_{q_{23}} = L_2 \sin(q_2 + q_3)(L_4 m_4 + L_4 m_5 - d_4 m_4)(\dot{q}_1 - \dot{q}_0 + \dot{q}_2 + \dot{q}_3) + L_2 m_5 \sin(q_2 + q_3 - q_4)(L_5 - d_5)(\dot{q}_1 - \dot{q}_0 + \dot{q}_2 + \dot{q}_3 - \dot{q}_4) - L_2 d_3 m_3 \sin(q_2)(\dot{q}_1 - \dot{q}_0 + \dot{q}_2) + L_4 m_5 \sin(q_4)(L_5 - d_5)(\dot{q}_1 - \dot{q}_0 + \dot{q}_2 + \dot{q}_3 - \dot{q}_4) - L_4 m_5 \sin(q_4)(L_5 - d_5)(\dot{q}_1 - \dot{q}_0 + \dot{q}_2 + \dot{q}_3)$$

$$C_{q_{24}} = L_2 \sin(q_2 + q_3)(L_4 m_4 + L_4 m_5 - d_4 m_4)(\dot{q}_1 - \dot{q}_0 + \dot{q}_2 + \dot{q}_3) + L_2 m_5 \sin(q_2 + q_3 - q_4)(L_5 - d_5)(\dot{q}_1 - \dot{q}_0 + \dot{q}_2 + \dot{q}_3 - \dot{q}_4) + L_4 m_5 \sin(q_4)(L_5 - d_5)(\dot{q}_1 - \dot{q}_0 + \dot{q}_2 + \dot{q}_3 - \dot{q}_4) - L_4 m_5 \sin(q_4)(L_5 - d_5)(\dot{q}_1 - \dot{q}_0 + \dot{q}_2 + \dot{q}_3)$$

$$C_{q_{25}} = -L_2 m_5 \sin(q_2 + q_3 - q_4)(L_5 - d_5)(\dot{q}_1 - \dot{q}_0 + \dot{q}_2 + \dot{q}_3 - \dot{q}_4) - L_4 m_5 \sin(q_4)(L_5 - d_5)(\dot{q}_1 - \dot{q}_0 + \dot{q}_2 + \dot{q}_3 - \dot{q}_4)$$

$$
\begin{aligned}
C_{q_{31}} = {} & L_2 d_3 m_3 \sin(q_2)(\dot{q}_0 - \dot{q}_1) - L_2 \sin(q_2 + q_3)(\dot{q}_0 - \dot{q}_1) \\
& * (L_4 m_4 + L_4 m_5 - d_4 m_4) - L_1 \dot{q}_0 \sin(q_1 + q_2 + q_3)(L_4 m_4 \\
& + L_4 m_5 - d_4 m_4) + L_1 d_3 m_3 \dot{q}_0 \sin(q_1 + q_2) - L_2 m_5 \sin(q_2 \\
& + q_3 - q_4)(L_5 - d_5)(\dot{q}_0 - \dot{q}_1) - L_4 m_5 \sin(q_4)(L_5 - d_5) \\
& * (\dot{q}_1 - \dot{q}_0 + \dot{q}_2 + \dot{q}_3 - \dot{q}_4) - L_1 m_5 \dot{q}_0 \sin(q_1 + q_2 + q_3 - q_4) \\
& * (L_5 - d_5) + L_4 m_5 \sin(q_4)(L_5 - d_5)(\dot{q}_1 - \dot{q}_0 + \dot{q}_2 + \dot{q}_3)
\end{aligned}
$$

$$
\begin{aligned}
C_{q_{32}} = {} & L_2 \sin(q_2 + q_3)(\dot{q}_0 - \dot{q}_1)(L_4 m_4 + L_4 m_5 - d_4 m_4) \\
& - L_2 d_3 m_3 \sin(q_2)(\dot{q}_0 - \dot{q}_1) + L_2 m_5 \sin(q_2 + q_3 - q_4)(L_5 \\
& - d_5)(\dot{q}_0 - \dot{q}_1) + L_4 m_5 \sin(q_4)(L_5 - d_5)(\dot{q}_1 - \dot{q}_0 + \dot{q}_2 \\
& + \dot{q}_3 - \dot{q}_4) - L_4 m_5 \sin(q_4)(L_5 - d_5)(\dot{q}_1 - \dot{q}_0 + \dot{q}_2 + \dot{q}_3)
\end{aligned}
$$

$$
\begin{aligned}
C_{q_{33}} = {} & L_4 m_5 \sin(q_4)(L_5 - d_5)(\dot{q}_1 - \dot{q}_0 + \dot{q}_2 + \dot{q}_3 - \dot{q}_4) \\
& - L_4 m_5 \sin(q_4)(L_5 - d_5)(\dot{q}_1 - \dot{q}_0 + \dot{q}_2 + \dot{q}_3)
\end{aligned}
$$

$$C_{q_{34}} = C_{q_{33}}$$

$$C_{q_{35}} = -L_4 m_5 \sin(q_4)(L_5 - d_5)(\dot{q}_1 - \dot{q}_0 + \dot{q}_2 + \dot{q}_3 - \dot{q}_4)$$

$$
\begin{aligned}
C_{q_{41}} = {} & L_4 m_5 \sin(q_4)(L_5 - d_5)(\dot{q}_1 - \dot{q}_0 + \dot{q}_2 + \dot{q}_3) \\
& - L_2 \sin(q_2 + q_3)(\dot{q}_0 - \dot{q}_1)(L_4 m_4 + L_4 m_5 - d_4 m_4) \\
& - L_2 m_5 \sin(q_2 + q_3 - q_4)(L_5 - d_5)(\dot{q}_0 - \dot{q}_1) \\
& - L_4 m_5 \sin(q_4)(L_5 - d_5)(\dot{q}_1 - \dot{q}_0 + \dot{q}_2 + \dot{q}_3 - \dot{q}_4) \\
& - L_1 m_5 \dot{q}_0 \sin(q_1 + q_2 + q_3 - q_4)(L_5 - d_5) \\
& - L_1 \dot{q}_0 \sin(q_1 + q_2 + q_3)(L_4 m_4 + L_4 m_5 - d_4 m_4)
\end{aligned}
$$

$$
\begin{aligned}
C_{q_{42}} = {} & L_2 \sin(q_2 + q_3)(\dot{q}_0 - \dot{q}_1)(L_4 m_4 + L_4 m_5 - d_4 m_4) \\
& + L_2 m_5 \sin(q_2 + q_3 - q_4)(L_5 - d_5)(\dot{q}_0 - \dot{q}_1) \\
& + L_4 m_5 \sin(q_4)(L_5 - d_5)(\dot{q}_1 - \dot{q}_0 + \dot{q}_2 + \dot{q}_3 - \dot{q}_4) \\
& - L_4 m_5 \sin(q_4)(L_5 - d_5)(\dot{q}_1 - \dot{q}_0 + \dot{q}_2 + \dot{q}_3)
\end{aligned}
$$

$$C_{q_{43}} = C_{q_{44}} = C_{q_{33}}, \quad C_{q_{45}} = C_{q_{35}}$$

$$
\begin{aligned}
C_{q_{51}} = {} & L_2 m_5 \sin(q_2 + q_3 - q_4)(L_5 - d_5)(\dot{q}_0 - \dot{q}_1) \\
& + L_1 m_5 \dot{q}_0 \sin(q_1 + q_2 + q_3 - q_4)(L_5 - d_5) \\
& - L_4 m_5 \sin(q_4)(L_5 - d_5)(\dot{q}_1 - \dot{q}_0 + \dot{q}_2 + \dot{q}_3)
\end{aligned}
$$

$$
\begin{aligned}
C_{q_{52}} = {} & L_4 m_5 \sin(q_4)(L_5 - d_5)(\dot{q}_1 - \dot{q}_0 + \dot{q}_2 + \dot{q}_3) \\
& - L_2 m_5 \sin(q_2 + q_3 - q_4)(L_5 - d_5)(\dot{q}_0 - \dot{q}_1)
\end{aligned}
$$

$$C_{q_{53}} = L_4 m_5 \sin(q_4)(L_5 - d_5)(\dot{q}_1 - \dot{q}_0 + \dot{q}_2 + \dot{q}_3)$$

$$C_{q_{54}} = C_{q_{53}}, \quad C_{q_{55}} = 0$$

Gravitational Torque Elements

$$G_{q_1} = -g \sin(q_0)(L_1 m_2 + L_1 m_3 + L_1 m_4 + L_1 m_5 + d_1 m_1)$$

$$G_{q_2} = -g \sin(q_0 - q_1)(L_2 m_3 + L_2 m_4 + L_2 m_5 + d_2 m_2)$$

$$G_{q_3} = d_3 g m_3 \sin(q_1 - q_0 + q_2)$$

$$G_{q_4} = g \sin(q_1 - q_0 + q_2 + q_3)(L_4 m_4 + L_4 m_5 - d_4 m_4)$$

$$G_{q_4} = g m_5 \sin(q_1 - q_0 + q_2 + q_3 - q_4)(L_5 - d_5)$$